The Thesis Committee for Mark Hamilton Duncan
Certifies that this is the approved version of the following thesis:

The Northeastern Gulf of Mexico: Volcanic or Passive Margin? Seismic Implications of the Gulf of Mexico Basin Opening Project

APPROVED BY
SUPERVISING COMMITTEE:

Supervisor:

(Gail Christeson, Supervisor)

(Harm van Avendonk, Co-Supervisor)

(Sean Gulick)

(Kyle Spikes)

The Northeastern Gulf of Mexico: Volcanic or Passive Margin? Seismic Implications of the Gulf of Mexico Basin Opening Project

by

Mark Hamilton Duncan, B.S.

Thesis

Presented to the Faculty of the Graduate School of

The University of Texas at Austin

in Partial Fulfillment

of the Requirements

for the Degree of

Master of Science in Geological Sciences

The University of Texas at Austin

May, 2013

Acknowledgements

I would like to thank both my advisors, Gail Christeson and Harm van Avendonk for their support over the past two years in the states and abroad. I would like to thank Sean Gulick and Kyle Spikes for taking the time to review this thesis and for their support throughout. Several fellow graduate students including Bobby Reece, Dan Eakin, Ryan Lester, Drew Eddy, Maureen Levoir, and Sebastian Ramirez have also been integral parts of my success in the completion of this thesis. As always, I thank above all else those that gave everything so that I might have this opportunity.

Abstract

The Northeastern Gulf of Mexico: Volcanic or Passive Margin? Seismic Implications of the Gulf of Mexico Basin Opening Project

Mark Hamilton Duncan, MS Geosciences

The University of Texas at Austin, 2013

Supervisors: Gail Christeson, Harm Van Avendonk

The Gulf of Mexico Basin Opening project (GUMBO) is a study of the lithological composition and structural evolution of the Gulf of Mexico (GoM) that uses Ocean Bottom Seismometer (OBS) data from four transects in the Northern GoM. I examine 39 OBS shot records in the easternmost transect for shear wave arrivals and pick shear wave travel times from the 11 usable records. I then carry out a tomographic inversion of seismic refraction travel times. I use the resulting shear-wave velocity model in conjunction with a previously constructed P-wave model to examine the relationship between Vp and Vs. I compare velocities in the sediment and basement with empirical velocities from previous studies for the purpose of constraining lithological composition below the transect and make an interpretation of the structural evolution of the eastern GoM.

The seismic velocities for crust landward of the Florida Escarpment are consistent with normal continental crust. Seaward of the Escarpment, velocities in the upper oceanic crust are anomalously high (Vp = 6.5 – 7 km/sec; Vs = 4.0 – 4.6 km/sec). A possible

explanation for this observation is that GoM basalt formation consisted of basaltic sheet flows, forming oceanic crust that does not contain the vesicularity and lower seismic velocities found in typical pillow basalts. Increased magnesium and iron content could also account for these high velocities.

Seismic refraction and reflection data provide a means of investigating the nature of the Moho in the northeastern GoM. I use a finite difference method to generate synthetic record sections for data from eight instruments that are part of the two easternmost GUMBO seismic lines (lines 3 & 4). I then vary the thickness of the Moho in these synthetic models and compare the results with the original receiver gather to examine the effects this variability has on amplitudes.

The data from the instruments chosen for these two lines are representative of continental and transitional crust. The finite difference models indicate that the Moho beneath GUMBO 3 is ~1500 m thick based on the onset and amplitudes of PmP arrivals. All five instruments display consistent results. The instruments along GUMBO 4 suggest a Moho almost twice as thick as GUMBO 3 on the landward end of the transect that grades into a Moho of similar thickness (1750 m) in the deep water GoM. The three instruments used to model the Moho in this area show that the Moho ranges from ~1750 to 3500 m in thickness. The sharper boundary beneath continental crust in GUMBO Line 3 supports other evidence that suggests magmatic underplating and volcanism in the northern GoM during the mid-Jurassic. The thicker Moho seen on the landward end of GUMBO Line 4 that is overlain by continental crust was likely unaffected by GoM rifting. Therefore, the Moho beneath the Florida Platform might be as old as the Suwannee Terrane, and complex Moho structure is not uncommon for ancient continental crust.

Table of Contents

List of Tables

List of Figures

CHAPTER 1: GEOLOGIC BACKGROUND

Introduction

The opening of the Gulf of Mexico (GoM) Basin is a relatively enigmatic subject. Thick sediment cover, a lack of magnetic anomalies that show the age and direction of seafloor spreading, as well as a lack of deep geophysical data that detail the nature of the basement make the study of GoM structural evolution very challenging.

Detrital zircon analysis, heat flow measurements, and the principles of superposition have led to a general consensus that the rifting that resulted in the basin opening initiated in the mid to late Jurassic, ~165 Ma, and that the Yucatan block rotated counter-clockwise away from North America by ~40 – 60 degrees (Pindell and Dewey 1982; Bird, 2005; Mann, 2007; Stern and Dickinson, 2010; Urban et al., 2011) by ~140 Ma. Reconstructions show that the northwestern edge of what is now the Yucatan peninsula was attached to North America until the early Jurassic (Pindell and Dewey 1982; Bird, 2005; Stern and Dickinson, 2010). The rotational opening suggests that at least one dextral strike slip boundary must have existed in the mid to late Jurassic on the eastern coast of present day Mexico to accommodate this motion (Ross and Scotese, 1988; Stern and Dickinson 2010). The Yucatan is considered to contain key pieces of information to understanding the tectonic motion of the GoM (Pindell and Dewey, 1982). It is an independently moving block of continental crust that is shown in paleo-reconstructions to have been wedged between North and South America prior to continental breakup (Ross and Scotese, 1988). Subsequently, the Yucatan block moved southward in the same direction as South America, and then it rotated counter clockwise as a result of the opening of the western GoM (Pindell and Dewey, 1982; Ross and Scotese, 1988; Urban et al., 2011).

The Louann and Campeche salt formations are considered vitally important in understanding tectonic motion and timing in the GoM. It is believed that the top of these salt deposits must not be much older than late Callovian in age (Salvador, 1987). If they were, they would have been eroded or washed away through dissolution before the overlying upper Jurassic age Norphlet clastics were deposited (Imlay, 1980). The deposition of this salt is the result of the initial flooding of seawater during the early expansion of the GoM, followed by a period of lowered sea level and evaporation. The presence of these salt deposits suggests that seawater circulation was limited in the early GoM, however, it is tentatively suggested that oceanic crust formed in the middle of these deposits, splitting them into the two north and south segments (Sawyer et al., 1991). The east-west trending spreading center in the GoM is inferred by observing that these salt formations are of the same age and divided into north and south provinces (Sawyer et al., 1991).

Important questions remain related to how this motion was accomplished, e.g. where is the Euler rotation pole for basin opening in the western GoM and how does this translate to opening in the east? What roles do oceanic crust and surrounding blocks of continental crust play in structural evolution? What are the causes for the initiation of continental rifting and the underlying mechanisms responsible for spreading in both the eastern and western GoM? Was the margin cold and devoid of magma, or was extension accompanied by volcanic activity? This study focuses specifically on the nature of rifting in the eastern GoM.

Mechanisms for Basin Opening

BACKGROUND

There are many studies that use various methods to constrain the timing and kinematics relating to paleo-reconstructions of the GoM basin opening as well as several different hypotheses as to the cause of the opening itself (Bird et al., 2005; Fillon, 2007; Mann, 2007; Mickus et al., 2009; Stern and Dickinson, 2010; Urban et al., 2011). The red beds of the Eagle Mills formation are potentially a resultant formation from the Late Triassic Texas uplift (Dickinson et al., 2010) and a strong indicator for the onset of initial rifting in the GoM ~200 Ma (Salvador, 1987). The timing for basin opening has primarily been constrained using detrital zircons from Mesozoic sedimentary rocks, as well as heat flow measurements and superposition of stratigraphic layers that suggest that GoM seafloor spreading began ~165 Ma and ended between 140 and 145 Ma (Pindell and Dewey 1982; Salvador, 1987; Ross and Scotese, 1988; Galloway, 2008; Stern and Dickinson, 2010). Later stratigraphic units show rifting of the GoM margins (Norphlet clastics, Buckner, Smackover and Cotton Valley deposits ~155 – 140 Ma) overlying evaporates that suggest initial flooding in the GoM (Louann Salt ~165 Ma). Finally cooling and subsidence increased sedimentation rates and allowed for episodes of large carbonate deposits (Sligo, James, Stuart City deposits ~130 – 100 Ma) along the rim of the modern GoM (Galloway, 2008).

Paleo-reconstructions show that the GoM is the result of continental rifting and short-lived seafloor spreading prior to the complete breakup of Pangaea (Ross and Scotese, 1988; Pindell et al., 2009). Several studies have come to similar conclusions and extend these ideas, attributing the cessation of sea floor spreading to interactions between North America, South America, and Mexican terranes (Mann, 2007; Urban et al., 2011). These ideas vary only slightly with regard to fault placement and complexity and show that the basin opening is just one piece of a very complicated story of Caribbean tectonic evolution.

PREVIOUS STUDIES

Bird et al. (2005) argue that a late Jurassic mantle plume generated hotspot tracks on both the North American plate and the Yucatan Peninsula tectonic block during basin opening. Gravity anomalies form two separate tracks that mirror each other along the inferred spreading center in the western GoM. The westward motion of the plate relative to the hotspot, concurrent with the spreading of oceanic crust to the North and South could certainly account for the gravity anomaly pattern presented by Bird et al. (2005). It is important to note however, that even if these gravity anomalies are the result of a small hotspot, the plume, according to the timing by Bird et al. (2005), would be far younger than the initial rift basins and is not a likely cause for rifting.

The hotspot-track argument is supported by plate kinematic models and a rotation pole consistent with 20 degrees of counter-clockwise rotation through sea floor spreading (Bird et al., 2005). A hot spot in the western GoM would suggest that deep mantle material had in fact become buoyant at some time prior to spreading, and would support the findings of later studies (Dickinson, 2009; Mickus et al., 2009) that suggest that the northwestern GoM is a volcanic rifted margin that grades into an amagmatic rifted margin east of Louisiana. However, the notion that the eastern GoM is nonvolcanic (Dickinson, 2009; Mickus et al., 2009) is disputed by data that include seaward dipping reflectors (SDRs) south of the Florida panhandle below the Louann salt deposits, and a crustal geometry of the margin that is not consistent with passive continental boundaries (Imbert, 2005).

Stern and Dickinson (2010) classify the Gulf of Mexico as a Jurassic back-arc basin (BAB) in that it is an extensional basin formed by sea floor spreading, occurring behind an active magmatic arc and within the lifespan of that magmatic arc. The BAB hypothesis is supported by the observation that a short lifespan (10 to 30 Ma) is characteristic of back-arc basins, but the reason for such short lifespans is unknown (Stern and Dickinson, 2010). This short lifespan is supported by the evidence seen in currently active back-arc basins with an average age of 11.2 +/- 8.9 Ma and in extinct back-arc basins with an average duration of 12.5 +/- 4.7 Ma (Stern and Dickinson, 2010). One of the main differences between BAB basalt and mid-ocean ridge basalt is that BAB basalt is generated from a magma source that is more hydrated (1.14% versus < 0.5%) than the mantle beneath mid-ocean ridges (Stern and Dickinson, 2010). A depletion of the supply of hydrated mantle beneath the basin is one explanation of the ephemeral nature of BAB spreading (Stern and Dickinson, 2010). The rationale behind the BAB hypothesis is that subduction causes extension in the overriding plate and, therefore, provides a mechanism for rifting in the GoM.

SYNTHESIS

Assuming the paleo-reconstruction that places the Yucatan block between South America and North America with a rotation angle of 40 to 60 degrees is accurate, the hypothesis that the GoM is a back-arc basin and formed purely by slab rollback from the north-south trending Nazas arc is unlikely based on the unvarying observation that every intra-ocean back-arc basin we can easily identify spreads along a ridge axis that is parallel to the subduction trench. The BAB in the sea of Japan, the Mariana Trough, and the Lau Basin for example all are within a few degrees of parallel with their corresponding subduction trench. On the other hand, continental BABs are not restricted by this geometry. The Columbia River Flood Basalt province is such an example, which displays back-arc erratic subaerial extrusion of basalt in which the geometry is bound by continental topography (Smith, 1992; Stern and Dickinson, 2010). Furthermore, trench rollback and consequential thinning of the crust cannot be ignored because of the numerous subduction zones that have existed in this region since the Triassic. This complexity means that although the GoM is unlikely to be a well-defined intra-oceanic BAB due to the geometry of the spreading axis, crustal thinning due to slab rollback coupled with voluminous back-arc igneous activity can certainly be held accountable for aiding in the thinning of continental crust, subaerial extrusion of basalts, and eventual opening of the basin (Stern and Dickinson, 2010).

It is difficult to place Florida in plate reconstructions, though it is clear that it bordered both South America and western Africa prior to the breakup of Pangea (Mann, 2007, Urban et al., 2011). Nonetheless, the Florida Platform is a critical part of understanding tectonic evolution in the GoM. Based on plate reconstructions it has been speculated that Florida overlies a major discontinuity that has been interpreted as a left – lateral transform plate boundary during the Jurassic, connecting the Atlantic and GoM spreading centers (Klitgord et al., 1984). The Florida Straits Block is thought to have moved with South America and Africa in the initial rifting stages of the GoM along this hypothesized transform boundary to the southeast relative to the Suwannee Terrane, which lies to the north of the boundary (Ross and Scotese, 1988; Heatherington et al., 1999, 2003).

The Suwannee Terrane extends from southern Georgia and Alabama to the middle of peninsular Florida, the basement of which is composed of both mafic and felsic material that are constrained by K-Ar analyses to be early Jurassic in age (Heatherington et al., 2003) The analyses of drillhole samples in southern Florida are also Jurassic age, but differ geochemically and are thought to have been derived from a mantle plume associated with early Jurassic magmatism (Heatherington et al., 1999, 2003).

Sediments overlying the continental shelf offshore Florida as well as along the entire rim of the GoM are composed of both clastics and carbonate sequences (Salvador, 1987; Galloway, 2008). Rift-related sedimentary sequences overlie the Suwannee Terrane to the north of the trans-Florida Jurassic transform boundary. The basins that are filled with these Jurassic-age sediments are likely the result of failed rifts prior to sea-floor spreading in the Atlantic (Heatherington et al., 1999, 2003). Northern Florida contains sedimentary rocks of Paleozoic age, which are overlain by Triassic clastics in the South Georgia Basin (Klitgord et al., 1984). The carbonate rim along the Florida Platform is a late Jurassic to mid Cretaceous feature which is the result of a long term transgression as the GoM subsided (Galloway, 2008).

CHAPTER 2: CONSTRUCTING A SHEAR WAVE VELOCITY MODEL FOR GUMBO LINE 4

Methods

DATA ACQUISITION

The Gulf of Mexico Basin Opening marine seismic refraction project (GUMBO) began in the Fall of 2010 with the purpose of constraining crustal lithology as well as furthering our understanding of rifting and structural evolution in the northern Gulf of Mexico. This study includes four transects from ~300 km to just over 500 km long, using Ocean Bottom Seismometer (OBS) deployments and air-gun seismic sources aboard the R/V *Iron Cat*. OBS spacing for transects in the eastern GoM is 12 km with a time sampling interval of 5 ms and a shot spacing of 150 m. The data used in this study are from the easternmost line (line 4), which extends ~500 km southwest from offshore Steinhatchee Florida near Gainesville (Fig. 2-1). The transect is perpendicular to the Florida Escarpment and parallels the approximate rift direction of the eastern GoM (Fig.2-1).

SHEAR WAVE PICKS

Fig. 2-1 shows the locations of the 43 OBSs that were deployed along GUMBO line 4. Thirty-eight instruments recorded data of sufficient quality, and eleven recorded clear shear-wave arrivals representing crustal refractions and Moho reflections (OBSs 407, 418, 419, 422, 424, 425, 426, 429, 434, 435, and 441). Four separate channels record data for each OBS. These include the vertical motion component (channel 1), two perpendicular horizontal motion components (channels 2 and 3), and the hydrophone, or water pressure component (channel 4). Channels 1, 2 and 3 consistently display the clearest and earliest shear wave arrivals. I pick all SmS (Moho reflections) and Sg (crustal refractions) arrivals with an assigned uncertainty of ~150 ms from either channel 2 or channel 3 in each instrument using the SEG-Y file format and applying a reduction velocity of 4 km/sec (vertical axis = time(sec) – distance(km)/4(km/sec)). This reduction velocity displays shear waves as sub-horizontal in the shot record, with SmS arrivals having slightly higher velocities than those of Sg arrivals. Figure 2-2 shows these picked arrivals in the vertical channel data as well as the horizontal channel data for a single OBS (OBS 425, picks were made in channel 2). Figure 2-3 shows the horizontal channel data for OBS 425 with zoomed in sections for the Sg and SmS picks.

RAY TRACING AND TOMOGRAPHIC INVERSION

To create a starting shear-wave seismic velocity model I use a previously constructed P-wave model (Fig. 2-4) as a base, and define a linear relationship between observed P-wave velocities and empirical Vp-Vs relationships from Brocher (2005) (Vs = a + b*Vp). I assume P-S wave conversion occurs at the seafloor, and modify the parameters a and b in the sediment layer. I keep a and b fixed in all other layers, and trace ray paths from source to receiver through the starting model. By doing this, I obtain misfits between the calculated and observed arrival times that vary among different instruments. Because these misfits vary from continental to oceanic regimes, I divide

GUMBO Line 4 into three lateral sections (0-75 km, 75 – 225 km, 225 – 500 km) with *a* and *b* parameters that best fit each section. I then trace ray paths through this model following the methods of Van Avendonk et al. (2004). I apply linearized tomographic inversions (Van Avendonk et al., 2004; Eddy et al., 2013, GRL in press) to update the basement and sediment layers of the velocity model based on the difference between observed and calculated shear wave arrival times (figures 2-5 and 2-6). This inversion is regularized such that it solves for the model with the smoothest Vp/Vs ratio while fitting the shear-wave travel time data (Eddy et al., in press). I trace ray paths through the updated velocity model and iterate the tomographic inversion. I repeat this process until the calculated arrivals fit within the previously determined uncertainty (~150 ms of the observed arrivals). The final result is the shear-wave velocity model shown in figure 2-7. There are no clear shear-wave arrivals from refractions or reflections in the sediment layer observed in the OBS data, which may be due to velocity differences that do not allow for shear-wave conversion. Therefore, sediment velocities are not constrained by GUMBO 4 shear-wave arrivals other than by the ray paths that have turned in the basement. Consequently, I cautiously interpret sediment lithologies using observed P-wave velocities along with the average corresponding shear-wave velocities for vertical raypaths through the sediment layer.

Results

Interpreting lithology requires a comparison between the velocities estimated in the GUMBO 4 models with seismic refraction data and empirical seismic velocities measured in various laboratory experiments (Hamilton, 1979; Christensen, 1996;

Brocher, 2005; Bakulin et al., 2008). To make this comparison I select locations for four vertical profiles in the final velocity models (150, 240, 320 and 425 km from the landward end of GUMBO 4 - figures 2-4 and 2-7). These locations represent sections of continental, transitional and oceanic crust, and they are situated in the areas that contain the most abundant ray coverage in the sediment and basement. The profiles are digitized at 1 km intervals to a depth of 25 km (continental crust) or to the crust-mantle boundary (transitional and oceanic crust). The shear-wave velocities from the vertical profiles are plotted as a function of P-wave velocities in figures 2-8 and 2-9.

Because of the large number of arrivals, ray coverage in the P-wave velocity model is extensive, covering nearly the entire section along GUMBO 4 to the Moho (Fig. 2-4). The shear wave velocity model is less encompassing, covering ~50% of the crustal layer due to the fewer shear wave arrivals in the shot records (Fig. 2-7). Where there is ray coverage in the shear model, however, crustal velocities are well constrained by the tomographic inversion, and my lithological interpretation will focus on these regions. Because there are no shear-waves that turn in the sediments along GUMBO 4, the interpretation of sediment lithology will be made with the understanding that sediment velocities are not well constrained compared to crustal velocities.

The velocity results for the crustal layer of GUMBO 4 are plotted in figure 2-8. The gray line running through the center of the graph is an empirical fit from laboratory measurements of common lithologies in sediments and continental and oceanic crust (Brocher, 2005). This fit is compiled from a dataset consisting of wireline borehole logs, vertical seismic profiles, laboratory measurements, and *in situ* estimates from seismic tomography models. I use this fit as a general guideline for a broad interpretation of lithologies along GUMBO Line 4.

Ranges for expected lithologies along GUMBO Line 4 are plotted with error bars in figures 2-8 and 2-9. These ranges were obtained from previous studies that measured velocities through both crustal rocks and through sediments (Hamilton, 1979; Christensen, 1996; Bakulin, 2008). Measurements were made by applying a range (200 MPa to 1000 MPa) of hydrostatic confining pressures to rocks in laboratory experiments (Christensen, 1996 - Fig. 2-8), a range of vertical and horizontal effective stresses (0 – 4000 psi) from wells in GoM sediments (Bakulin, 2008 – Fig. 2-9), and by computing average *in situ* velocities in twenty different sea floor locations (Hamilton, 1979).

The far northeastern vertical profile from GUMBO Line 4 (red squares in figures 2-8, 2-9) is taken 150 km from the landward end of the transect, crossing what is expected to be normal continental crust ~20 km in thickness, overlain by a ~9 km thick sediment layer. These velocities cluster in a very distinct group (figures 2-8, 2-9) (Vp = 6.0 – 6.7 km/sec; Vs = 3.8 – 4.0 km/sec) toward the upper (high Vs) bounds of the range of measured velocities of granodiorite and felsic granulite (Christensen, 1996). The transitional crust (green circles in figures 2-8, 2-9) 240 km from landward end of GUMBO 4) is consistent with the Brocher (2005) empirical fit and contains slightly higher P-wave velocities than the continental crust. The two vertical profiles that represent oceanic crust (profiles 3 and 4; 320 km and 425 km from the landward end of GUMBO 4 respectively) exhibit anomalously high P and S wave velocities in the upper crust (Vp = 6.7 – 7.0 km/sec; Vs = 3.9 – 4.2). Additionally, whereas P-wave velocities in the lower crust are consistent with typical oceanic gabbros (Vp = 7 – 7.1 km/sec), the shear velocities are anomalously high (Vs = 4.2 – 4.7 km/sec), effectively lowering the Vp/Vs ratio (Vp/Vs = 1.4 – 1.75 compared to typical oceanic gabbros with a Vp/Vs ratio of ~1.8 – 1.9) (Christensen, 1996).

The sedimentary layer of GUMBO 4 is characterized by higher velocities than the Brocher (2005) empirical fit. This difference is best shown in profile 1, where the results cluster in a group immediately to the right, but within the range of known average velocities of carbonate rocks (Hamilton, 1979; Vetrici, 1993) (Fig. 2-9). Sediment velocities from all four vertical profiles generally fall to the right of the Brocher (2005) empirical fit, suggesting a higher Vp/Vs ratio in the sediments. The misfit between profiles 2 and 3 and the Brocher (2005) empirical fit is significant in comparison to profiles 1 and 4. Additionally, the carbonate reef exhibits seismic velocities that differ significantly from clastic sediments (Fig. 2-9).

Discussion

The four vertical profiles examined in the velocity models represent sediments from the continental shelf and deep water GoM, as well as basement that includes continental crust from the Florida Platform, transitional crust, and oceanic crust from deep water GoM. Many of these shear-wave velocities are consistent with expected lithologies for their locations, while others are unusually high. These abnormal velocities that are estimated in the upper oceanic crust, along with observations that include margin geometry and sedimentation, shed new light on the structural evolution of the GoM and suggest two possibilities as to the nature of rifting and oceanic spreading in the eastern GoM. 1) The margin along the Florida Platform is volcanic in origin, and the oceanic crust in deep water GoM is the result of a deep magma source, i.e. a mantle plume which drove plate tectonics in the mid to late Jurassic. 2) The margin is the result of transform faulting, coupled with rifting due to far-field stresses as the western GoM opened. These far-field stresses then created a void for adiabatic decompression melting to take place with high temperature basalts ultimately filling the underlying void.

BASEMENT

The basement of the Florida Platform is represented by vertical velocity profile 1 (Fig. 2-8, 150 km). Though the S-wave velocities appear to be on the high end of the error bounds, both P and S-wave velocities are consistent with normal continental basement (Christensen, 1996). These velocities are expected as the west Florida Platform is composed of stranded blocks of crystalline continental crust (Klitgord et al., 1984).

The abnormally high velocities in the upper oceanic crust data suggest two possibilities: 1) low porosity in the basalt, or 2) mineral composition that is characteristic of basalt formed at high enough temperatures to incorporate greater concentrations of magnesium and iron (Eccles et al., 2009). The first possibility would likely be the result of the oceanic crust being made up of basaltic sheet flows, as opposed to typical upper oceanic crust composed of vesicular pillow basalts. The second possibility suggests that the parent magma of this oceanic crust was generated deep within the mantle, and that it is perhaps the product of active, plume-driven rifting.

GEOMETRY

The geometry of the transition from continental to oceanic crust (figure 2-4) is similar to that of a volcanic rifted margin. Figure 2-10 shows a schematic of a volcanic rifted margin based on data from the Gulf of Aden and the Atlantic margins (Menzies et al., 2002). When this figure is compared to the geometry in my velocity model, it can be seen that the distance over which the transitional crust extends in GUMBO 4 is similar, as is the general geometry of the margin though it is stretched slightly more than in the schematic covering ~150 km of lateral distance as opposed to ~100 km. The seismic velocities in the oceanic crust, however, are not completely consistent with a typical volcanic rifted margin. Though the upper oceanic crust displays anomalously high velocities, the lower oceanic crust displays velocities that are more typical of passive, non-volcanic margins. An alternative interpretation of this relatively narrow transition includes the removal of tensile strength from the margin. Potential mechanisms for this event include: 1) the presence of a significant strike slip component in the eastern GoM that has been shown to bisect peninsular Florida to the south of the Suwannee Terrane (Pindell and Dewey, 1982; Klitgord, 1984; Urban, 2011), or 2) an episode of intrusive diking that split the continental crust and forced it apart. Both of these events could also have occurred in succession, with the transform fault providing a weak area of lithosphere for diking to take place.

RIFTING AND SEA-FLOOR SPREADING

The question of whether rifting allows for plume activity or if plumes initiate rifting is still a subject of debate (Hooper, 1990; Menzies et al., 2002). It is understood, however, that the rifting of plate-driven margins is initiated by extensional forces followed by passive asthenospheric upwelling whereby melt generation is relatively shallow (Menzies et al., 2002). The inference of magnesium and iron enriched basalts beneath GUMBO 4 suggests that melt generation for oceanic crust in the eastern GoM was from a deeper source and the product of potentially high mantle temperatures. High

P and S-wave velocities are often attributed to plume and breakup-related thick mafic underplating (Gernigon et al., 2012) as well as subaerial extrusion of basaltic magma (Menzies et al., 2002; Imbert et al., 2005).

Seaward dipping reflectors (SDRs) have been seismically imaged in the eastern GoM beneath the Florida Escarpment (Imbert, 2005) and consist of two parallel belts 50 km wide and 150 km long, overlain by the Jurassic age Louann salt (Imbert et al., 2005, Stern and Dickinson, 2010). The presence of SDR's is a unique characteristic of volcanic rifted margins (Menzies et al., 2002). They support the idea of flood basalt formation, possibly above sea level, which would account for the high Vp and Vs in the shallow crust. The FUGRO MCS data that coincide with the GUMBO seismic lines do not image these reflectors well except for one on the landward most end of GUMBO Line 4 (figure 2-11), and a series of three on GUMBO Line 3 (figure 2-12) that are possibly part of the same band of SDR's imaged by Imbert (2005).

It is clear that the Gulf of Mexico is the result of continental breakup and short-lived seafloor spreading. The cause of the initiation of this rift can be explained by mantle upwelling combined with extensional forces from the initial stages of the breakup of Pangaea. What can be interpreted from the data in this study is that melt generation for oceanic crust in the eastern GoM was deep, producing basalt that can be attributed to a mantle plume as its source. Additionally, the high velocities from the upper oceanic crust must also be a result of lower porosity. These high velocities are most likely the result of basaltic sheet flows. It also suggests that the basalt has the potential to have formed subaerially, and that the eastern GoM may have been exposed during the incipient stages of rifting.

The Gulf of Mexico has been interpreted to have formed in several different ways. The most noteworthy of these hypotheses with respect to the data collected in this study include those that rely on mantle upwelling as well as extensional forces and basaltic flooding events as explanations for the onset of seafloor spreading (Imbert, 2005; Dickinson, 2009; Mickus et al., 2009,). The high velocities in the upper oceanic crust, the geometry of the margin, the presence of seaward dipping reflectors (Imbert, 2005), and short-lived sea floor spreading (Stern and Dickinson, 2010) are all indications that what has been interpreted as a volcanic rifted margin in the western GoM (Dickinson, 2009; Mickus et al., 2009) may in fact extend eastward to the Florida platform as far as GUMBO 4.

SEDIMENTATION

The Vp/Vs ratios for sediment on GUMBO 4 display an almost parallel fit with the observations of Brocher (2005). Figure 2-9 shows that Vp/Vs ratios from the carbonate platform (Profile 1, 150 km) plot laterally to the right of known carbonate velocities (Vp = 2.9 – 5.1; Vs = 1.6 – 2.8; Hamilton, 1979; Vetrici, 1993) meaning that Vp/Vs ratios are higher than average. According to velocity experiments by Aseffa, (2003) decreasing porosity in sediments causes both Vp and Vs to increase, though Vp increases twice as fast as Vs. Increasing effective pressure has the same effect on velocities (Vp increases twice as fast as Vs), particularly for pressures < 2 kb (Todd and Simmons 1972). The sediments in my analysis appear to have an increased effective pressure or decreased porosity compared to average sediments.

The carbonate rim along the Florida Platform is both broad and thick, covering just less than 300 km in lateral distance from the coastline with a thickness ranging from ~5 – 8 km (Fig. 2-4, 2-9 - Profile 1). This observation suggests that since the time that seawater flooded the eastern GoM, the margin has subsided as a result of cooling at a slow enough rate for carbonate organisms to survive throughout this time period and make up such a thick sedimentary layer.

OPENING THE EASTERN GOM

Throughout the Mesozoic, the formation of flood basalt provinces and episodes of mantle upwelling occurred frequently (Cox, 1980). These areas and the mantle plumes associated with them can be directly attributed to rifting and the breakup of Pangaea ~200 ma (Marzoli et al., 1999). The late Triassic - early Jurassic specifically was a period of widespread magmatism and extensional forces surrounding the study area. In addition, volcanic margins exist along the entire eastern seaboard of the United States (Marzoli et al., 1999), and their proximity to the eastern GoM is reason to believe that the forces responsible for them had similar effects on the eastern GoM. However, this notion is reached with the understanding that the time between the opening of the central Atlantic and the eastern GoM is extensive (~50 Ma).

On the other hand, the timing of the east-west separation of the Yucatan block and the Florida platform (~150 Ma) casts doubt on a connection between Late Triassic mantle plumes and one that could drive plate kinematics in the late Jurassic. This is not to say that a mantle plume did not exist in this area ~150 Ma, but plate reconstructions (Fig. 2-13) suggest that the area initially contained a significant amount of left lateral transform faulting as the Yucatan block separated from North America. Subsequently, the reconstructions show that the Yucatan block spread away from the Florida Platform as a result of far-field stresses and adiabatic decompression melting primarily from the rapid spreading in the western GoM.

Are far-field lithospheric stresses responsible for the onset of rifting in the eastern GoM, or is a deep-seated mantle plume and active volcanic rifting a more likely explanation? Higher-temperature low-porosity basalts, a narrow transitional crust, and the presence of seaward dipping reflectors in the eastern Gulf of Mexico imply that it is the result of active plume-driven rifting in the early Jurassic. However, the kinematic models of the opening of the GoM show that the Florida Escarpment initially accommodated strike-slip motion (Fig. 2-13), which is a potential explanation of the narrow transition zone. SDR's in the eastern GoM have only been reported on one set of seismic data (Imbert, 2001, 2005). These SDR's, while intriguing, are not necessarily the result of a mantle plume, but they are potentially pre-existing structures that are not indicative of an active volcanic margin.

I contend based on these lines of evidence that the eastern GoM is the result of rifting caused primarily by far-field stresses. Extensional forces caused by the rapid spreading of the western GoM forced the Yucatan Block away from the Florida Platform to the southwest along pre-existing zones of transform faulting. Following this seemingly passive rifting, adiabatic decompression melting, or the presence of a remnant mantle plume rose to fill the void underneath this rift. This high temperature magma resulted in low-porosity basaltic sheet flows rich in magnesium and iron. Resolution of the question regarding whether or not this buoyant mantle material could have driven rifting in the eastern GoM or passively filled a void in the lithosphere is unclear. However, transform faulting along the Florida Platform is likely (Klitgord et al., 1984) as is the presence of tensile stress perpendicular to these faults (Fig. 2-13). Therefore, it is not out of the question that extensional forces and active, plume-driven rifting could have occurred in conjunction with one another ~150 Ma.

Conclusions

1. The sediments that overlie the continental, transitional, and oceanic crust most likely consist of low-porosity or high-pressure turbidites and mudstones, along with a carbonate platform landward of the Florida escarpment.
2. This carbonate platform ranges from ~5-8 km in thickness. This thickness indicates that the eastern GoM went through a period of subsidence due to cooling rather than sediment loading.
3. The seismic velocities in the crust beneath the Florida platform are consistent with normal felsic crystalline basement.
4. The high P and S wave velocities along GUMBO line 4 suggest that the eastern Gulf of Mexico formed from large-scale mantle upwelling that resulted in a flood basalt event that may have been sub-aerial, forming what would become low-porosity, high-Mg and Fe oceanic crust.
5. The geometry of the ocean continent transition on GUMBO Line 4 near the Florida Escarpment is relatively narrow (~150 km), without a significant lateral section of crust that has been stretched to a thickness of ~10 km. Short lived rifting, combined with a significant strike-slip component along the Florida Platform may have removed any tensile stress in the margin and prevented extreme stretching of the lithosphere that is seen in typical amagmatic margins.
6. Because the deep structure along GUMBO Line 4 contains characteristics indicative of a volcanic rifted margin, i.e. significant mantle upwelling accompanied by flood basalt events, a narrow zone of transitional crust, and high P and S wave velocities in the upper oceanic crust, I have concluded that following a period of transform

faulting along the Florida Platform, the inferred volcanic rifted margin in the western GoM (Dickinson, 2009; Mickus et al., 2009) partly translates to the east, and is responsible for the high-temperature basalts found in the eastern GoM.

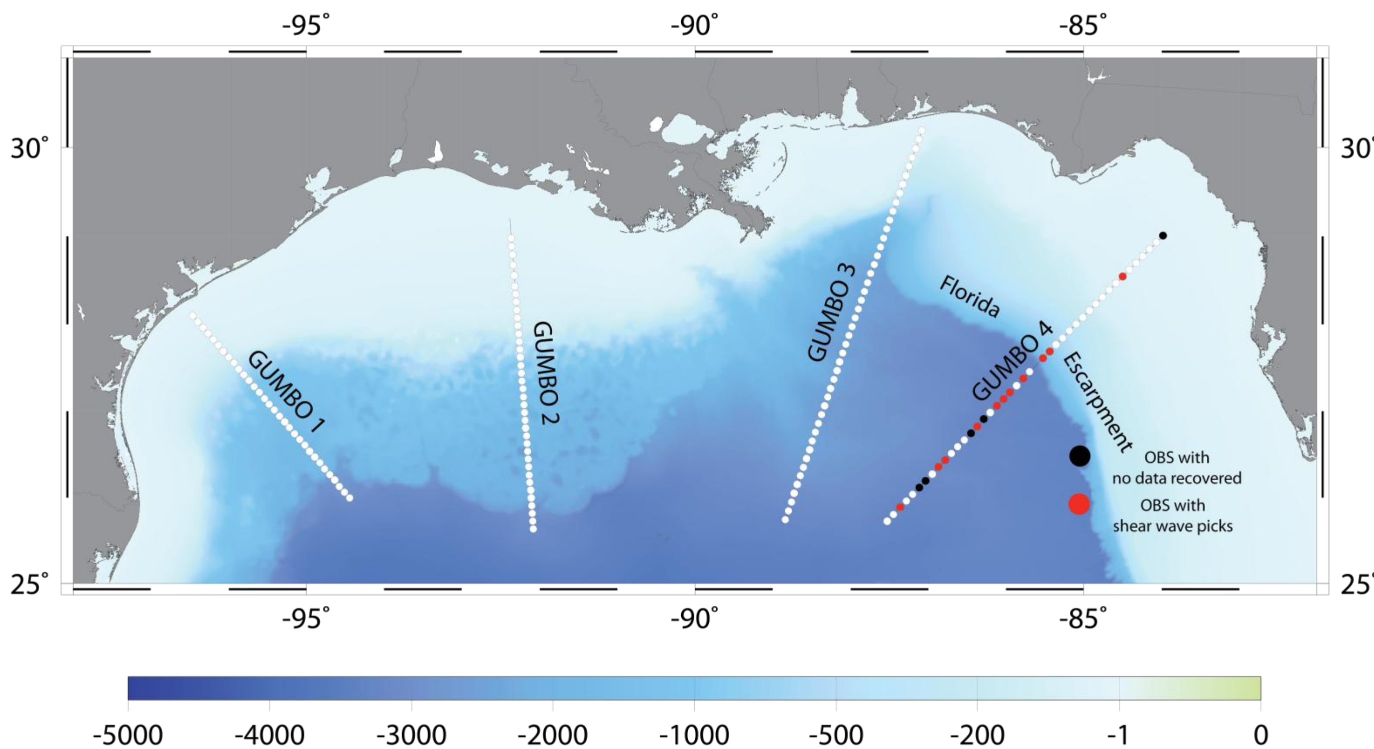

Figure 2-1: Study Area

GUMBO study area and locations of OBS deployments. Color coding is done only on line 4. White circles represent OBS with data recovered. Black circles represent OBS with no data recovered. Red circles represent OBS with shear wave data recovered.

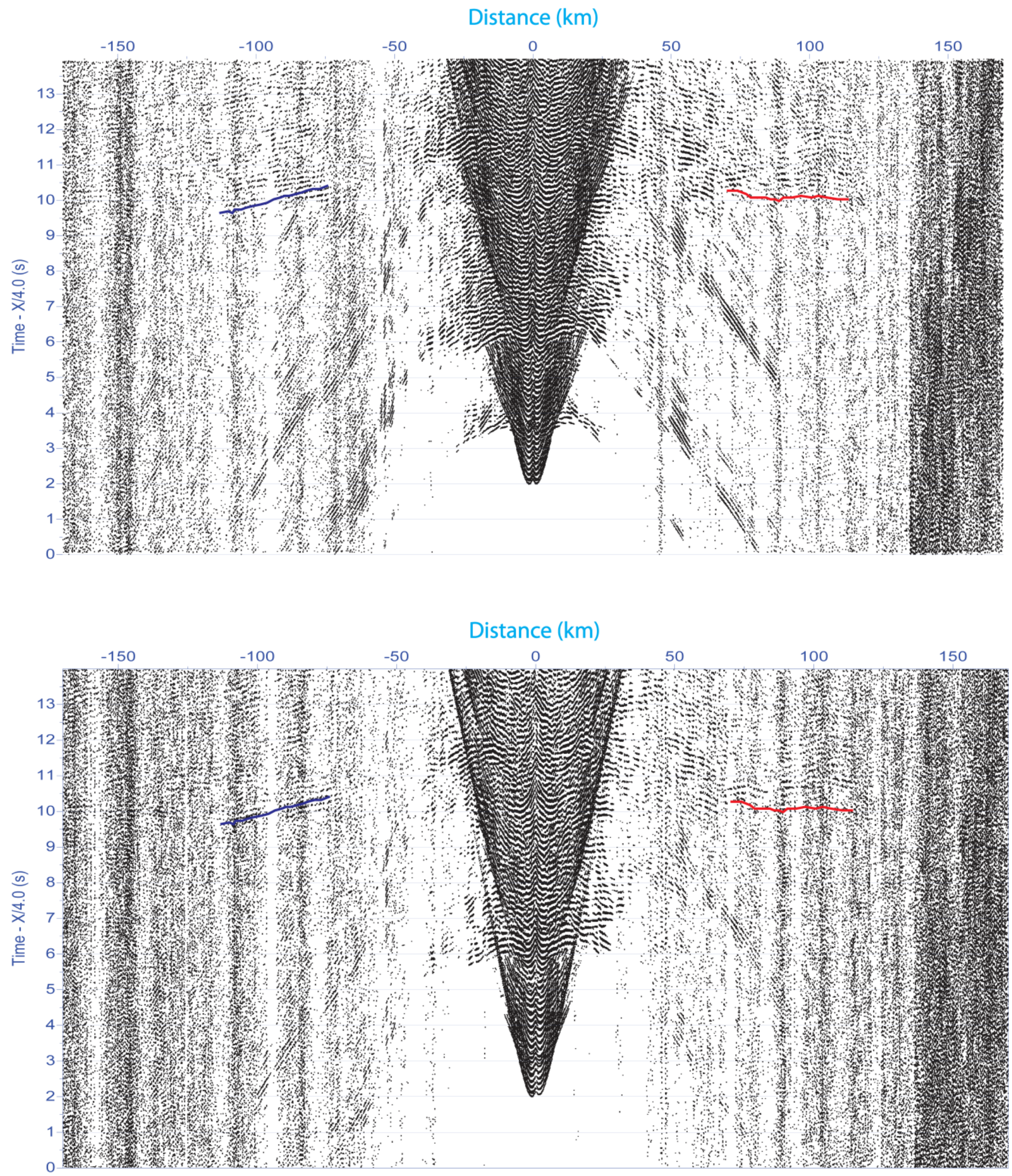

Figure 2-2: OBS Receiver Gathers

Vertical channel receiver gather for OBS 425 (top) and horizontal channel receiver gather (bottom) with Sg (red) and SmS (blue) picked arrivals. The data have been passed through a Butterworth filter, with a low cut of 3 Hz and a high cut of 15 Hz. The record sections are plotted with a reduction velocity of 4 km/s. An automatic gain control of 0.5 seconds has been applied.

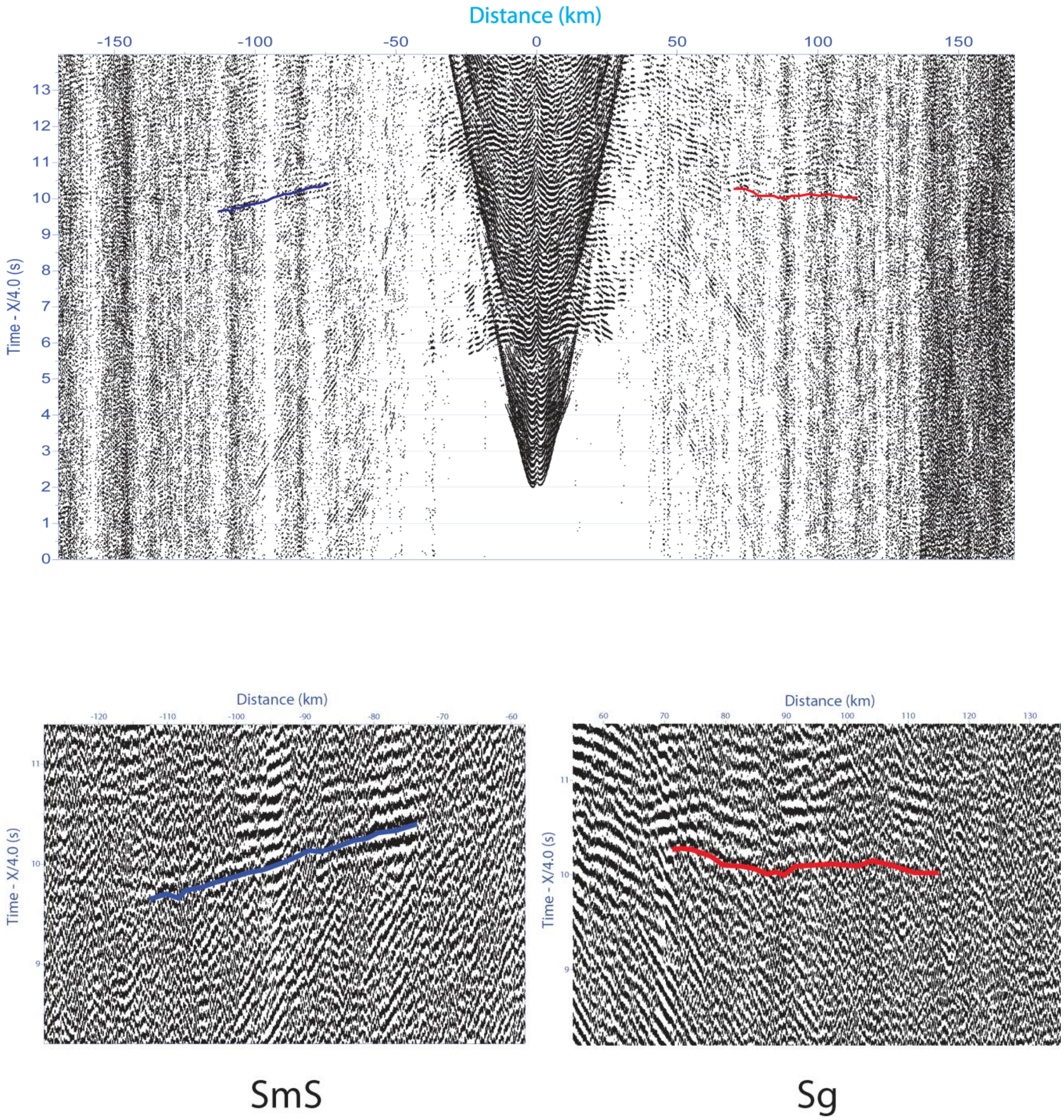

Figure 2-3: Shear Wave Arrivals

Horizontal channel for OBS 425 with zoomed in sections of picked Sg and SmS arrivals. The data have been passed through a Butterworth filter consisting of a low cut of 3 Hz and a high cut of 15 Hz. The record sections are plotted with a reduction velocity of 4 km/s and an automatic gain control of 0.5 seconds has been applied.

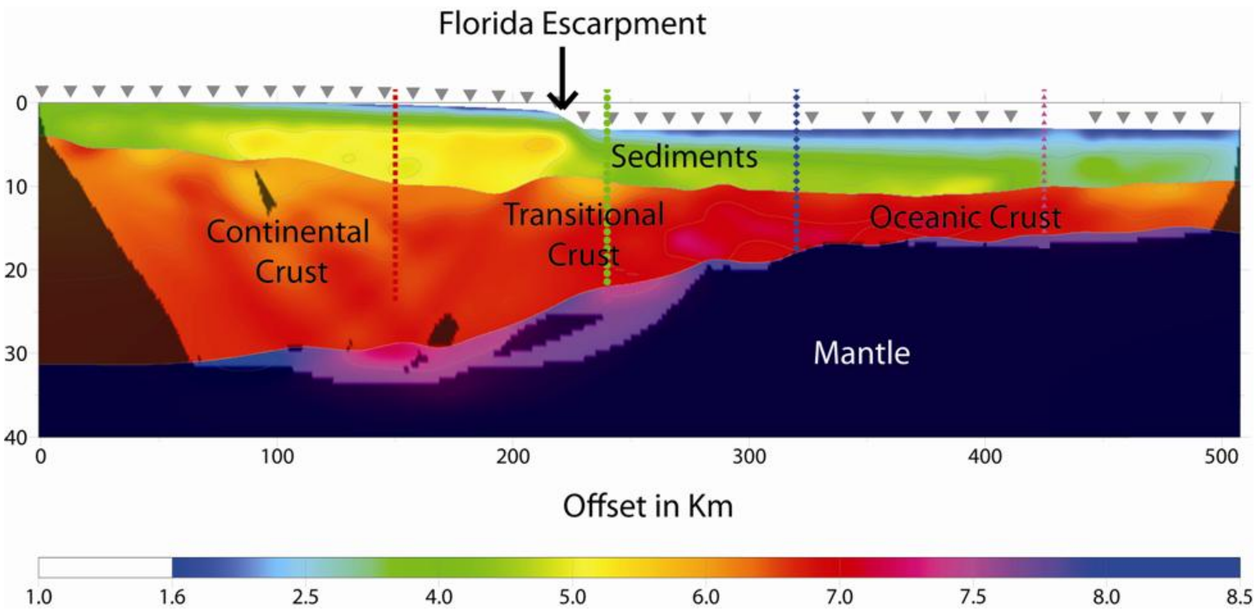

P-Wave Velocity (Km/s)

Figure 2-4: GUMBO 4 P-wave Velocity Model

P-wave velocity model showing the locations of the sediment layer; continental, transitional and oceanic crust; the mantle; Florida Escarpment, and locations of profiles plotted in later figures.

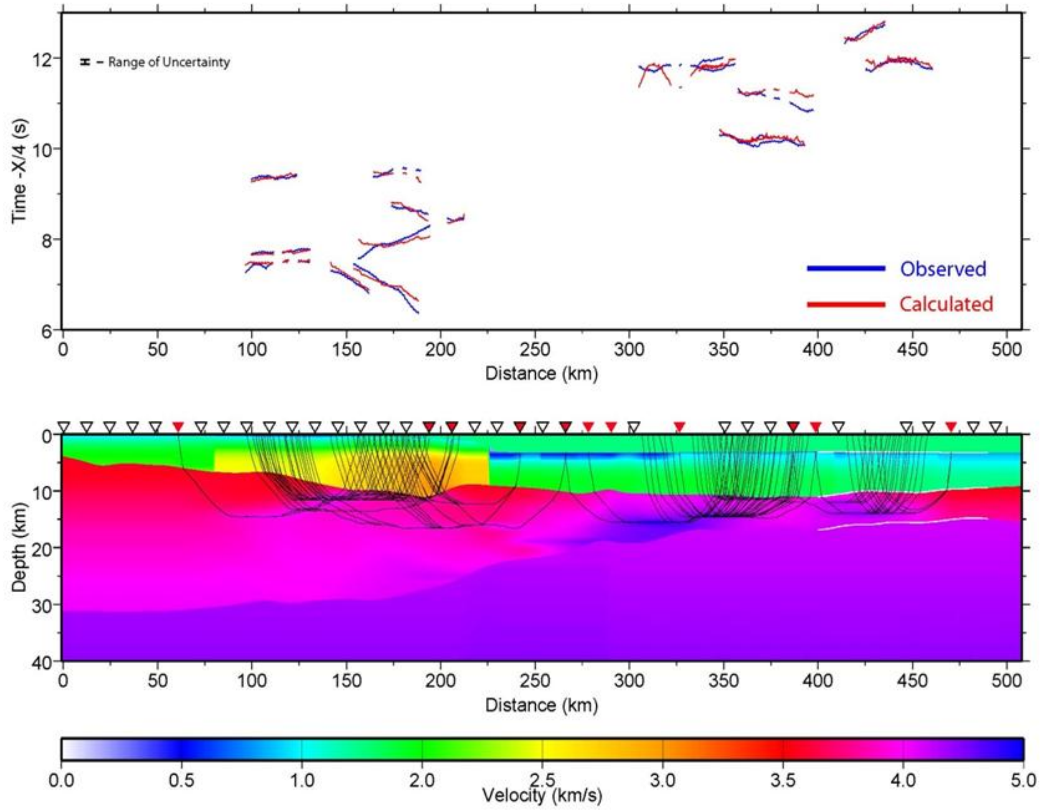

Figure 2-5: Sg Ray Tracing Diagram, GUMBO 4

Top: Phase 2 shear wave refractions in the basement, GUMBO line 4. Blue lines are observed Sg arrival times. Red lines are calculated Sg arrival times. Bottom: Red triangles are the locations of OBSs with picked Sg arrivals. Sg ray paths from source to receiver through velocity model.

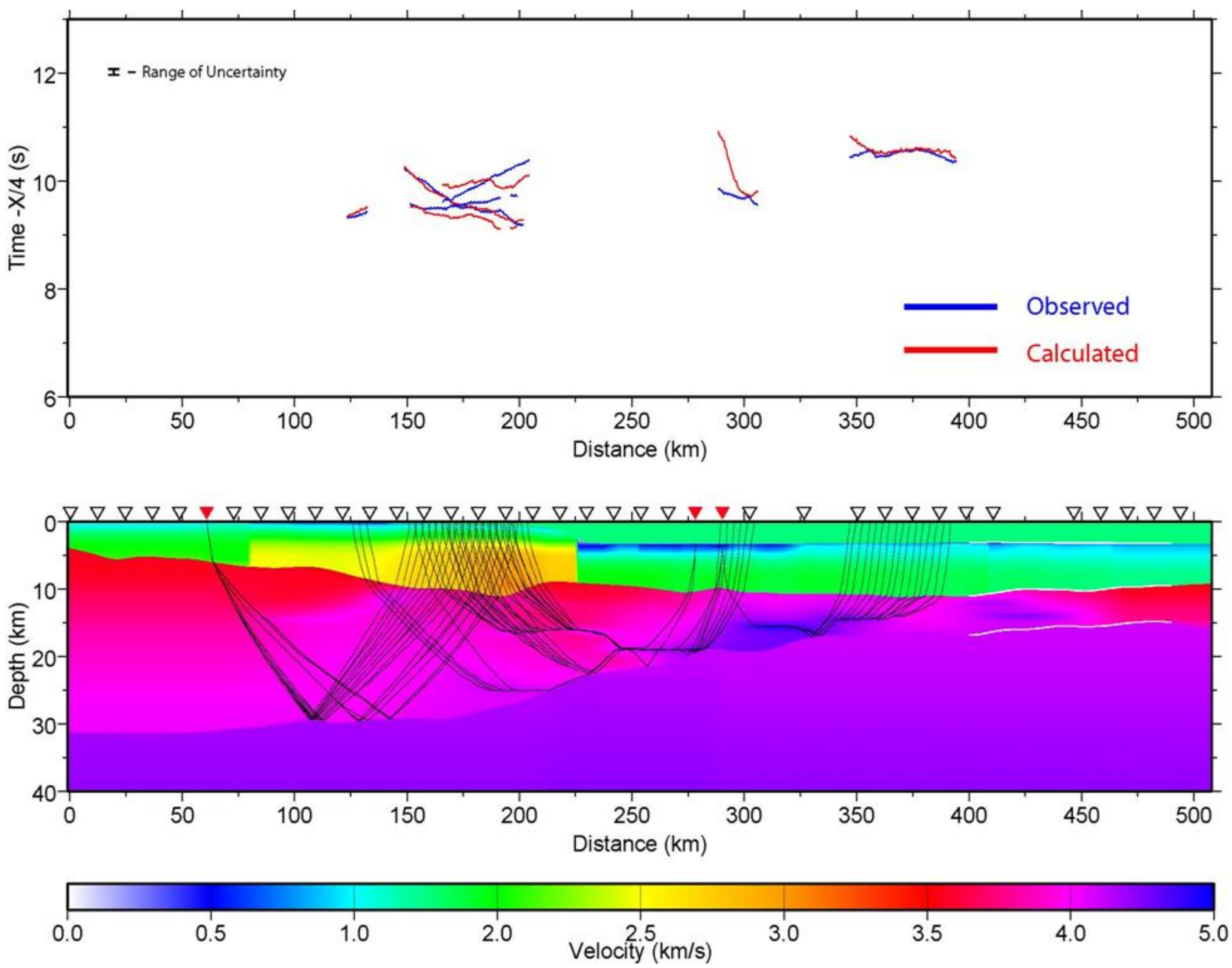

Figure 2-6: SmS Ray Tracing Diagram, GUMBO 4

Top: Phase -3 Reflections from the Moho, Gumbo line 4. Blue lines are Observed SmS arrival times. Red lines are calculated SmS arrival times. Bottom: Red triangles are the locations of OBSs with picked SmS arrivals. SmS ray paths from source to receiver through velocity model.

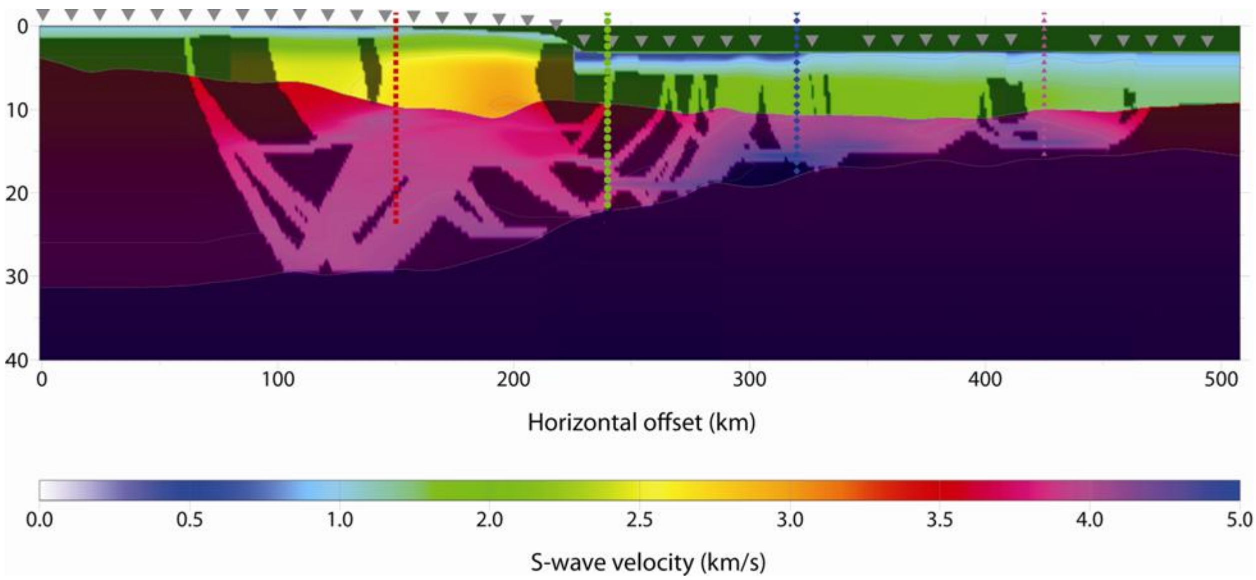

Figure 2-7: Shear wave Velocity Model, GUMBO 4

Final S-wave velocity model for GUMBO line 4. Dotted lines are at distances 150, 240, 320, and 425 km from the landward end of the transect and cover regions of continental, transitional, and oceanic crust. Highlighted regions are areas constrained by shear ray coverage.

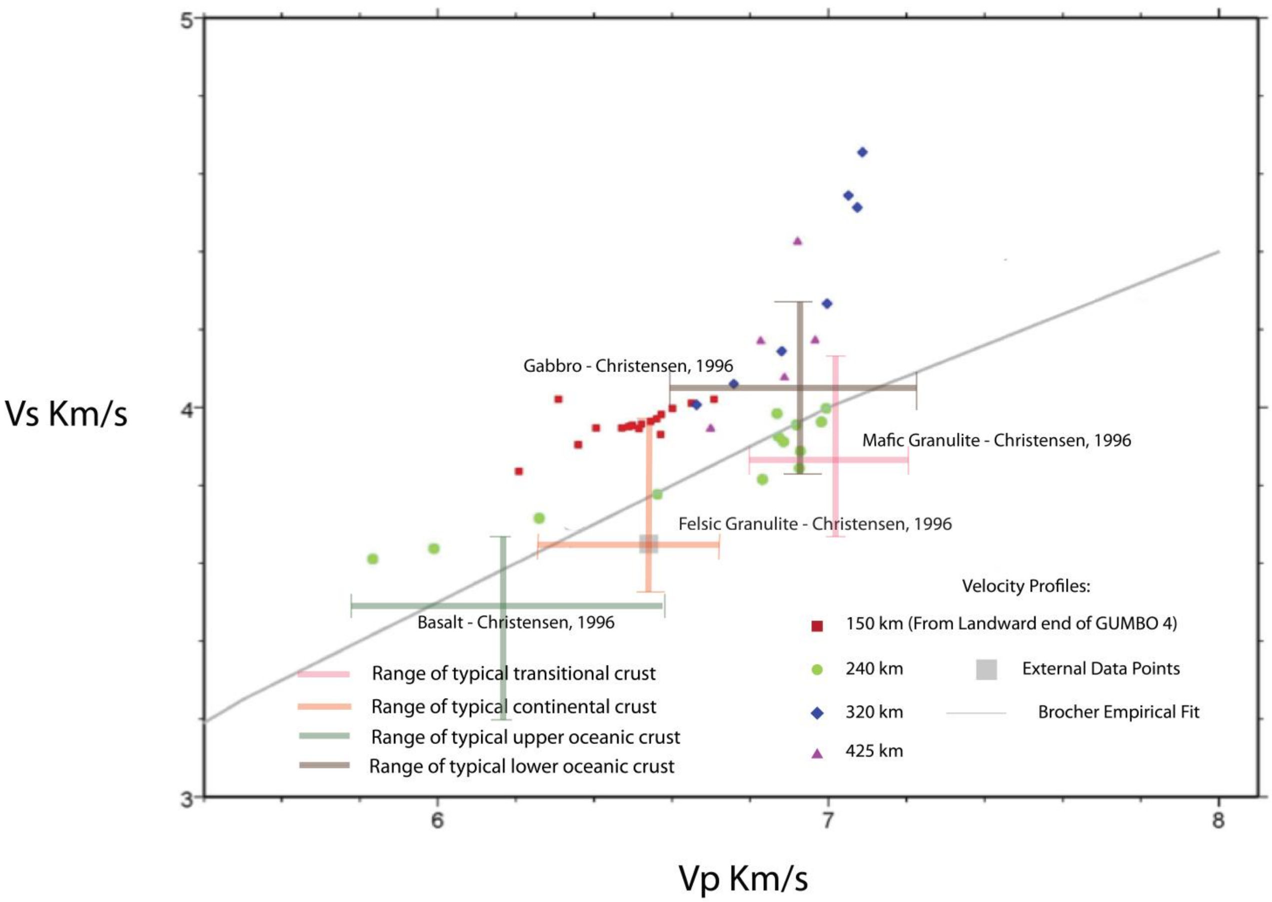

Figure 2-8: Crustal Velocities, GUMBO 4

Plots of crustal shear wave velocities as a function of compressional wave velocities for four vertical profiles (figures 4 and 7) along GUMBO line 4. The curve running through the center of the graph is an empirical fit for laboratory-observed velocities in common lithologies (Brocher, 2005). Ranges for observed velocities of specific rock types for typical continental, and upper and lower oceanic crust are shown in order to identify any inconsistencies between expected velocities in the GUMBO 4 data and that of previous studies.

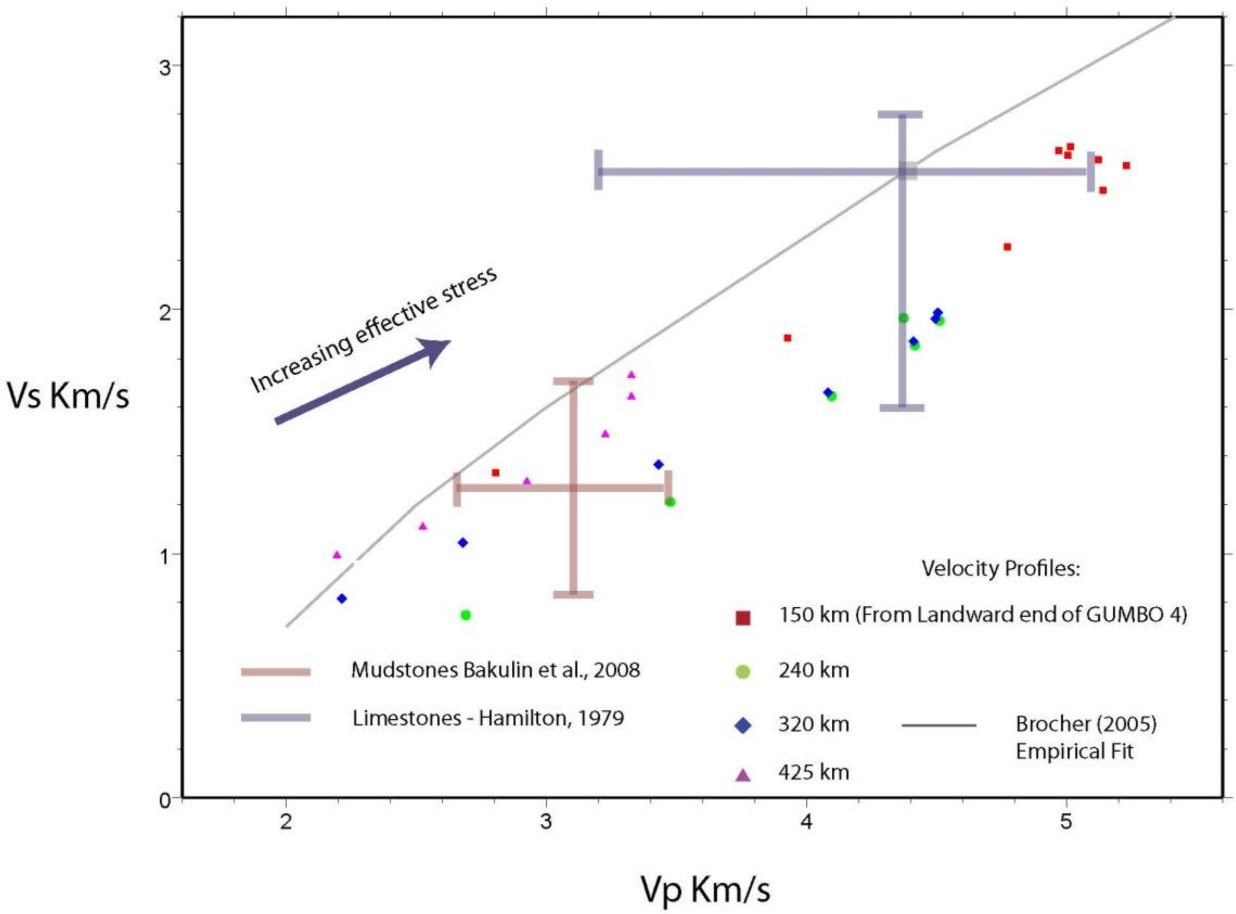

Figure 2-9: Sediment Velocities, GUMBO 4

Plots of sediment shear wave velocities as a function of compressional wave velocities for four vertical profiles (figures 4 and 7) along GUMBO line 4. The curve running through the center of the graph is an empirical fit for laboratory-observed velocities in common lithologies (Brocher, 2005). Ranges for observed velocities of specific rock types for typical mudstones and limestones are shown in order to identify any inconsistencies between expected velocities in the GUMBO 4 data and that of previous studies.

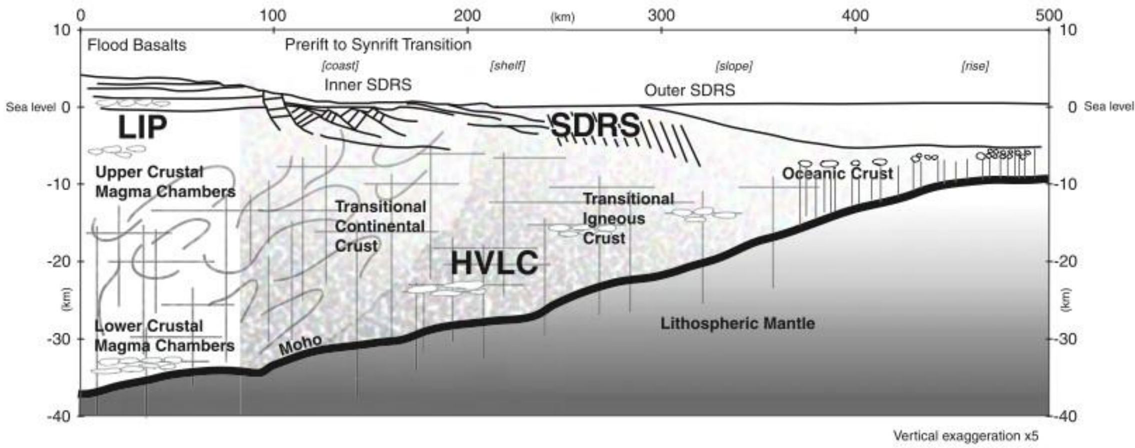

Figure 2-10: Volcanic Rifted Margin

Schematic of a volcanic rifted margin based on data from Ethiopia-Yemen and the Atlantic margins. From Menzies, 2002. The geometry of the margin along GUMBO 4 is very similar to typical volcanic rifted margins.

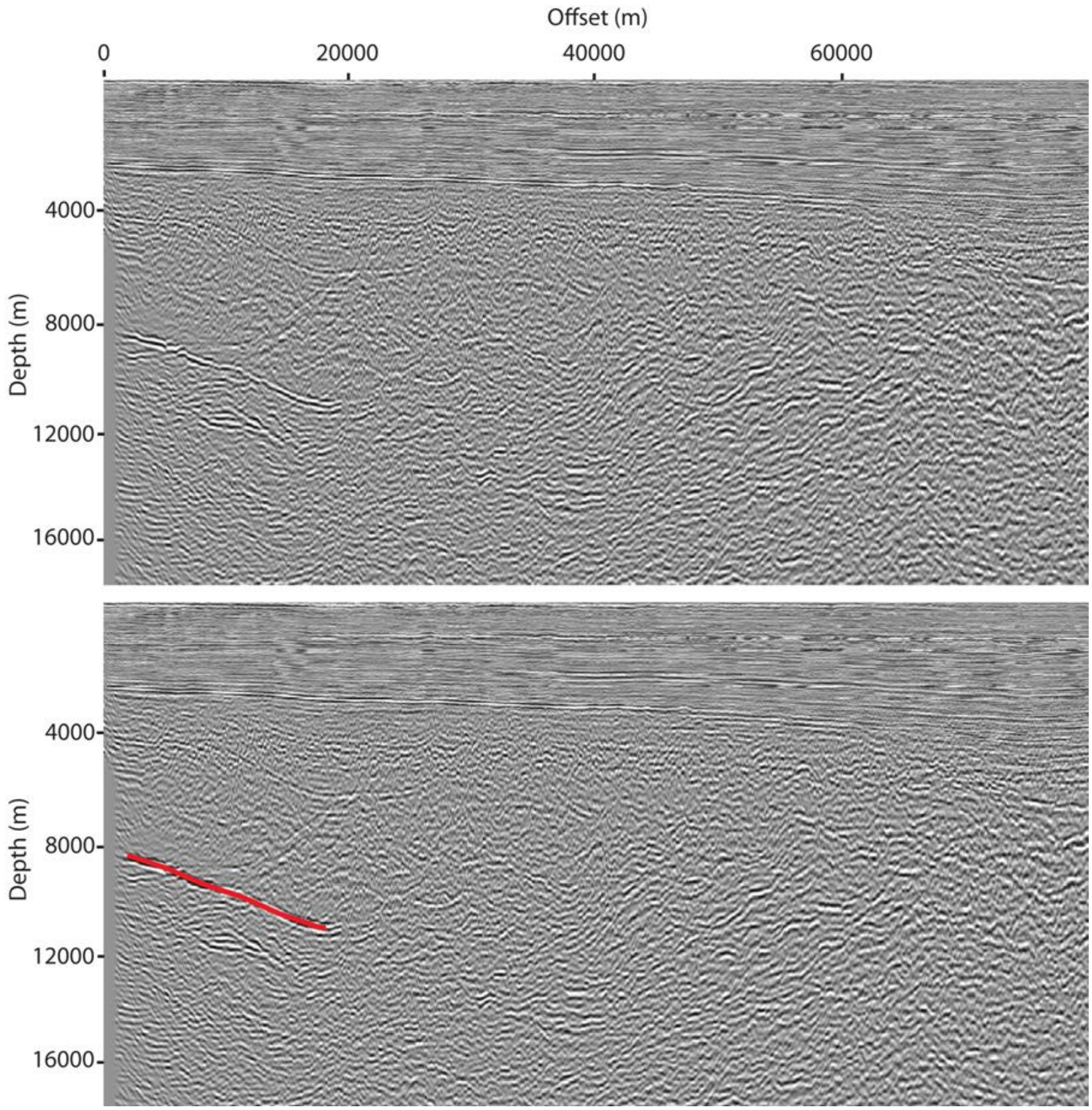

Figure 2-11: GUMBO 4 SDRs

Potential SDR on landward most end of GUMBO 4 SDR lies in the continental crust of the Florida Platform. SDR's are characteristic features of volcanic rifted margins.

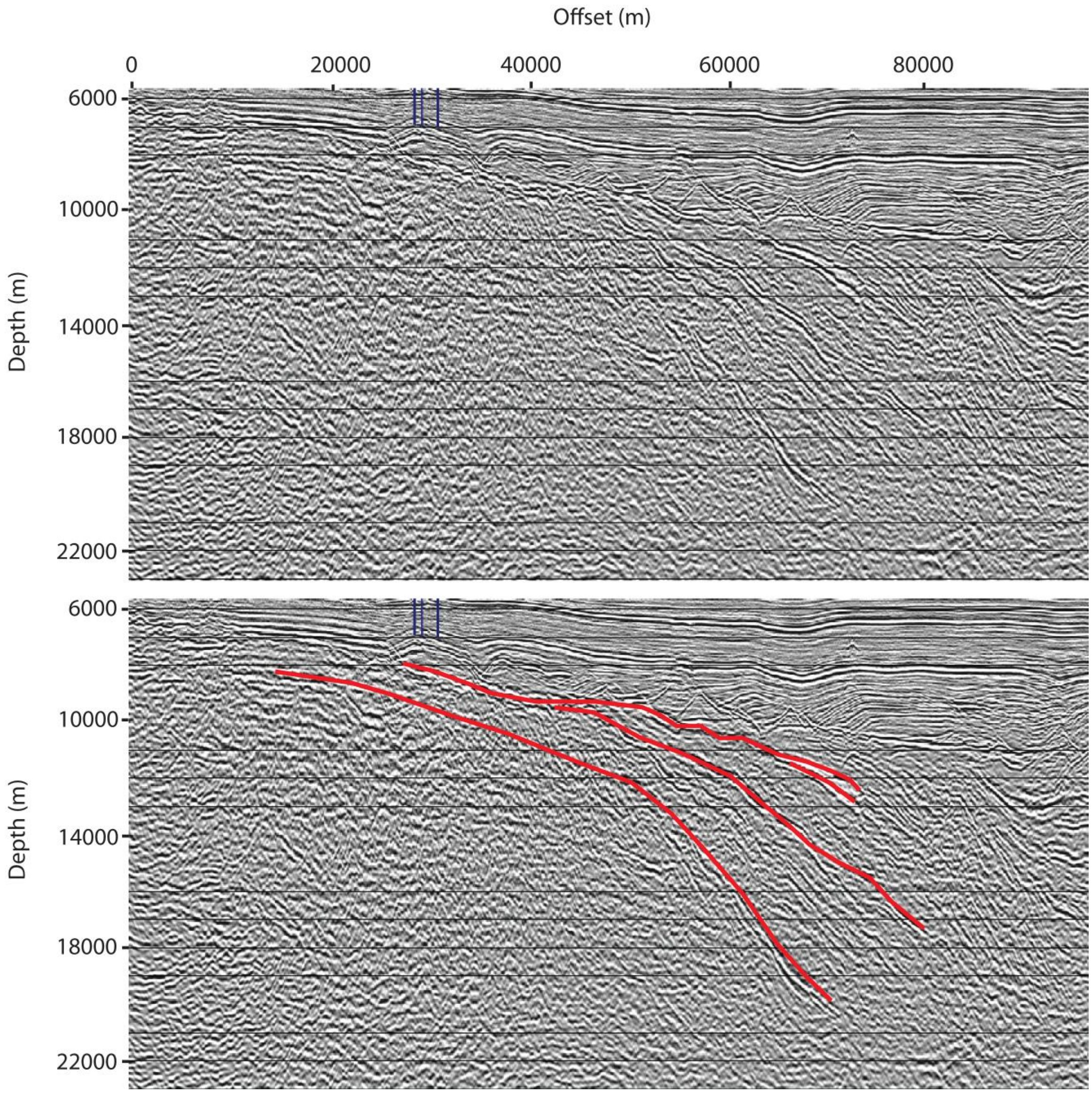

Figure 2-12: GUMBO 3 SDRs

Seaward dipping reflectors. SDRs lie within continental crust. These SDRs are potentially part of the same band imaged by Imbert (2005).

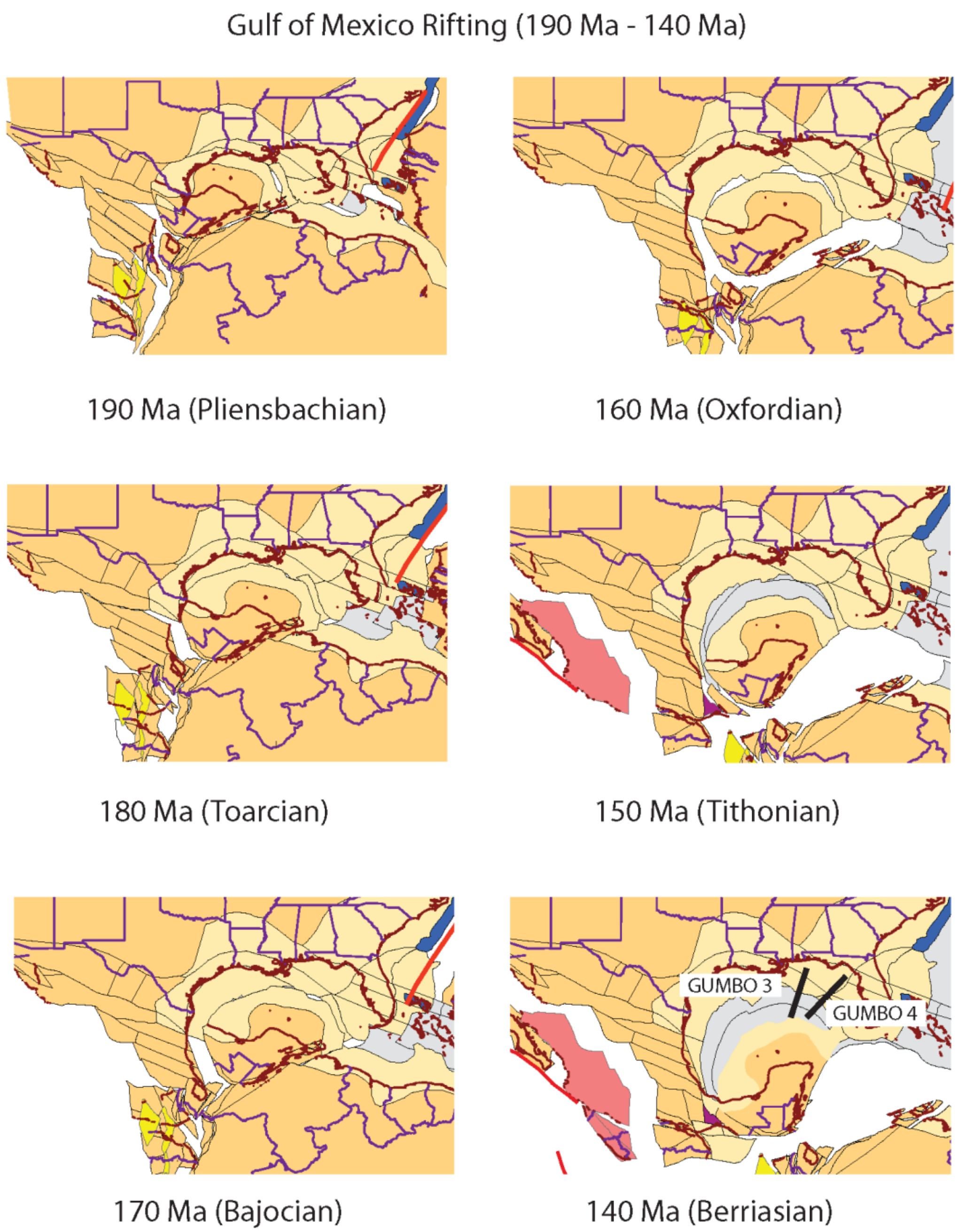

Figure 2-13: Gulf of Mexico Rifting 190 Ma to 130 Ma

Plate reconstruction of the GoM from 190 Ma to 140 Ma. This reconstruction shows sinistral transform faulting in the eastern GoM during early stages of rifting, followed by the onset of sea floor spreading in the east around 150 Ma. (Figure courtesy of Bud Davis, UTIG PLATES project, 2012).

CHAPTER 3: USING FORWARD MODELING TO INVESTIGATE THE NATURE OF THE MOHO IN THE EASTERN GULF OF MEXICO

Background

The Mohorovičić discontinuity, or Moho, is defined as the outermost boundary of a differentiated Earth, in which a large increase in seismic velocity takes place (from 6.7 – 7.2 km/s to 7.6 – 8.6 km/s) in both continental and oceanic regimes, indicating major changes in lithology and metamorphism to include chemistry, petrology, mineralogy, density, and rheology (Jarchow and Thompson, 1989; Oueity and Clowes, 2010). These changes represent the transition from mafic or felsic lower crustal material to ultramafic mantle material (Pallister and Hopson, 1981; Kennett et al., 2011). Characteristics such as thickness of the transition, velocity gradient, and heterogeneities in the Moho also vary geographically, and these traits may be dependent upon surrounding tectonics and geological history (Carbonell et al., 2002).

For the 104 years since its discovery in 1909, the Moho has been studied using a variety of seismic techniques, as well as with direct observation from ophiolites and uplifted mantle from continental regimes. The Moho was originally described as a first-order (zero thickness) discontinuous boundary between the lower crust and the upper mantle (Mohorovičić, 1910). This conclusion was reached based on the observation that there is a depth at which P-wave velocity increases extremely rapidly to 7.6 – 8.6 km/s (Mohorovičić, 1910). This sudden increase in seismic velocity suggested major changes in chemistry, petrology, mineralogy, density and rheology (Jarchow and Thompson, 1989; Oueity and Clowes, 2010). High-resolution images of the Moho have been acquired using seismic refraction and reflection techniques (e.g. Carbonell et al. 2002), and we now know that the physical nature of the Moho is far more complex than a single, first-order, uniform petrologic and seismic discontinuity. Several studies have shown that this transition zone is highly variable both laterally and vertically, exhibits thicknesses up to several kilometers, and contains a wide range of physical and petrologic characteristics (e.g. Pallister and Hopson, 1981; Jarchow and Thompson 1989; Kennett et al., 2011). Furthermore, the geologic history of the rock overlying the Moho may significantly affect the physical nature of this boundary (Carbonell et al., 2002).

Presently, even though high-resolution images of the Moho are available, the physical attributes of both the oceanic and continental crust-mantle transition are not only poorly understood as a whole, but also vary geographically. Ophiolites provide the only means of directly observing the oceanic Moho on the surface. Ophiolites are characterized by a transition from mafic to ultramafic lithologies over various thicknesses (Pallister and Hopson, 1981; Jarchow and Thompson, 1989). Less is known about the continental Moho due to the relative lack of exposure on the surface. The only observable evidence of continental Moho composition comes from small erupted xenoliths which seldom show any contact between lithologies (Jarchow and Thompson, 1989) and larger scale, although rarer uplifted exposures of the transition (Jarchow and Thompson 1989). These outcrops display lithological contacts, as well as the structural features of the crust-mantle boundary. The continental Moho has been seismically researched extensively, and has been shown to be more complex than a simple first order discontinuity, consisting of high and low velocity anastomosing layers and laminations that are laterally discontinuous (Hale and Thompson, 1982; Mooney and Brocher, 1987; Oueity and Clowes, 2010).

The tectonic evolution and geologic history of an area can be directly related to the nature of the crust-mantle transition (Carbonell et al., 2002). Tectonically, the GoM is the result of short lived sea floor spreading in the mid to late Jurassic. This seafloor spreading originated in the western GoM ~165 Ma, forcing the Yucatan block and South America to pull away from North America, followed by the Yucatan Block rotating as an independent piece of continental crust counterclockwise ~40 degrees (Pindell and Dewey 1982; Bird, 2005; Mann, 2007; Stern and Dickinson, 2010; Urban et al., 2011; Fig. 2-13). The spreading center then propagated eastward opening the eastern GoM and separating the Yucatan Block and the Florida Platform, beginning ~150 Ma.

Methods

The Moho structure is ubiquitous on the scale of the seismic wavelengths (~1 km) used for deep crustal study in the GUMBO project. Because of this ubiquity, ray tracing and tomography is an acceptable means of modeling for a large-scale velocity model such as in chapter 2. For investigating the finer details of subsurface geology, i.e. the nature of the crust–mantle transition, however, a method that can show detail on the scale of a single seismic wavelength, such as finite difference modeling is required. The purpose of this study is to use a finite difference approximation to the wave equation to create synthetic seismograms of mantle reflection and refraction arrivals, and to make an interpretation of the physical characteristics of the Moho in the northeastern GoM. This interpretation will allow for better understanding of the nature of rifting in the GoM during the Jurassic.

Previous studies have used several various forward modeling techniques to investigate the nature of the Moho in a variety of tectonic settings (Carbonell, 2002; Oueity and Clowes, 2010). These studies have examined different crust-mantle transitions, including 1) a layered transition, varying the thickness of the transition zone and the thickness of the internal layers (Oueity and Clowes, 2010); 2) a heterogeneous transition, varying thickness and velocity with laterally discontinuous layers or a lamellae structure (Oueity and Clowes, 2010); 3) a velocity gradient zone, which varies simply the thickness of the zone and the scale of the gradient (Oueity and Clowes, 2010; Carbonell et al., 2002); 4) a step discontinuity with topographic relief, varying the thickness and degree of roughness of the interface (Carbonell et al., 2002). Model 3 is the structure assumed for the purposes of this study.

I use a finite difference technique to approximate the two-dimensional acoustic heterogeneous wave equation, which is derived using Euler's relation and the equation of continuity (Keiswetter et al., 1995)

Euler's relation:

$$\frac{\partial v}{\partial t} + \frac{1}{\rho}\nabla p = 0$$

Equation of Continuity:

$$\frac{\partial p}{\partial t} + \rho c^2 \nabla\, v = 0$$

Where v is the particle velocity, p is the acoustic pressure, $\rho = \rho(x,z)$ is the density, and $c = c(x,z)$ is the velocity of the wave in the media (Keiswetter et al., 1995). Further explanation of the mathematics used for the finite difference code can be found in studies by Kelly et al. (1976) and Keiswetter et al. (1995).

I choose to model five representative instruments on GUMBO 3 and three instruments on GUMBO 4 that sample Moho of continental and transitional crust on each profile (Fig 3-1). I vary the transition thickness between 0 km (a sharp, first-order discontinuity) and 6 km in steps of 500 m to get a best fit PmP (compressional Moho reflections) and Pn (compressional mantle refractions). This thickness represents the vertical distance between the velocities estimated at the lowest point of the basement and the uppermost point of the mantle in the velocity model. The Moho velocity gradient is then a function of the difference in those two velocities divided by the thickness put in to the synthetic model. Once the best fit between the synthetics and the original is achieved, I vary the velocity gradient in the mantle from -0.001 km/sec/km to 0.004 km/sec/km in steps of 0.001 km/s/km for one instrument on each profile to determine the effect of mantle gradient on the Pn arrival.

Results

The onset of the PmP arrivals varies among instruments but is usually seen between 60 km and 70 km offset in GUMBO 3 data. GUMBO 4 data is more variable, with PmP onsets seen anywhere from 30 km to 90 km offset. PmP arrival times are consistently between 6 and 7 seconds in both GUMBO 3 and 4 (with a reduction velocity of 7) (Figs. 3-2 and 3-3).

Figures 3-2 and 3-3 show representative receiver gathers from each line with clear PmP and Pn arrivals. When the Moho thickness is increased, the PmP amplitudes in both of these instruments are attenuated beginning at near offsets. The amplitudes of the Pn arrival at far offsets in OBS 316 (Fig. 3-4) are also attenuated with increasing Moho thickness while near offsets are strengthened. Conversely, the amplitudes of the Pn arrival in OBS 404 (Fig. 3-5) are intensified with increasing thickness along the entire Pn arrival. This result is consistent between instruments in the same lines. Any PmP or Pn arrivals that appear in the data from OBSs 302, 305, 309, and 316 all attenuate with increasing Moho thickness. Likewise, all PmP arrival amplitudes from OBSs 404, 410, and 426 attenuate while Pn arrival amplitudes strengthen with increasing Moho thickness. Discrepancies among Pn arrivals are possibly the result of lateral heterogeneities within the mantle. PmP is therefore used as the primary means of interpreting Moho thickness beneath lines 3 and 4.

Mantle velocity gradient variability has far less of an effect on amplitudes. The mantle gradient for OBS 316 and OBS 404 is varied between -0.001 km/s/km and 0.004 km/s/km in increments of 0.001 km/s/km. Figure 3-5 shows the two extremes (-0.001 and 0.004 km/s/km) of this variation for OBS 316, and while the Pn arrival is affected very slightly, this difference is less than observed for models with different Moho thicknesses.

Table (3-1) gives the approximate thicknesses of the Moho for each instrument. It also lists the type of crust and the distances from the landward end of each line for Moho that is covered by ray paths in the velocity model. The P-wave velocity models for lines 3 and 4 (Fig. 3-7) show the lateral sections of Moho that are analyzed in this study. Additionally, the raypath diagrams for the representative instruments (Fig. 3-8, 3-9) show how raypaths cover these sections of Moho. The instruments from GUMBO Line 3 consistently suggest that the Moho along these sections is between 1500 meters to 2000 meters in thickness beneath continental and transitional crust. GUMBO Line 4 OBS data indicates a thicker Moho on the landward or northeast end of the transect (~3500 meters), which thins significantly (to ~1500 meters) as the overlying basement transitions from continental to oceanic crust.

Discussion

The results of this study show that Moho thickness variation has a distinct effect on both PmP and Pn arrival amplitudes. Changes in the mantle gradient affect Pn arrival amplitudes to a much lesser extent than changes in boundary thickness. Ray theory and Fermat's principal suggest that Pn rays would be concentrated with an increasing mantle gradient (Cerveny, 2001), and the rays would affect the synthetic seismograms more drastically by increasing Pn amplitudes. The synthetic models clearly show that this is not the case, as increasing the mantle gradient has little effect on Pn (Fig. 3-6). In contrast, distance for the onset of the PmP arrival, along with Pn amplitudes vary significantly with changes in Moho thickness in the synthetic models (Figs. 3-2, 3-3).

GUMBO LINE 3

The thin Moho beneath GUMBO Line 3 relative to line 4 is potentially a result of magmatic underplating from plume driven rifting that affected the transitional and continental crust beneath the transect. Due to the comparably low densities of crustal rocks, basaltic magma that is sourced from under continental regimes is often trapped at or near the Moho (Cox, 1993). This underplating would likely sharpen the contrast in composition between the crust and mantle, yielding the distinct 1500 to 2000 meter thicknesses shown by these synthetic models.

GUMBO LINE 4

The northeasternmost instrument in GUMBO Line 4 (OBS 404) provides data from the Moho underlying the continental basement of the Florida Platform. The synthetic seismograms show that the thickness of the transition between continental crust and mantle is ~3500 meters (Fig 3-3). A complex and thick Moho is common beneath old continental crust, and the Moho underlying the Florida Platform is comparable to the determined thickness of the 1.8 Ga transition zone (~3.3 km) beneath the Great Bear magmatic arc in northwestern Canada (Oueity and Clowes, 2010). The 3500 meter transition from crustal to mantle rocks suggests that the area was subject to long term tectonic processes that were capable of mixing mantle rock with the overlying crust. Quick et al., (1995) argue that this type of mixing can occur at subduction zones, where peridotites may mix with meta-sedimentary rock in the accretionary prism, creating a lamellae structure similar to that seen in sections of northwest Canada (Oueity and Clowes, 2010). Therefore, it can be inferred that the crust-mantle transition zone beneath this section of the Florida Platform was not affected by early Jurassic plutonism, and is as old as the Suwannee Terrane (~552 Ma) (Heatherington and Mueller, 2003). This result is consistent with the inference of a strike-slip component being responsible for the geometry of the margin discussed in Chapter 2.

OBS 426 is the furthest seaward instrument used for this study. It contains PmP arrivals from ray paths that travel both seaward and landward, and a Pn arrival from ray paths that travel landward in the velocity model. The results from applying Moho thickness variation to this instrument show that the Moho thins as the overlying basement transitions into oceanic crust (Table 3-1). This thinning is the expected result for a transition from normal continental crust to oceanic crust as the formation of younger oceanic crust from basaltic magma sharpens the boundary between mafic and ultramafic material.

NATURE OF RIFTING IN THE GOM

Chapters 1 and 2 discuss the potential mechanisms and forces responsible for rifting the eastern GoM. Velocity models, Vp/Vs ratios from that data, and conclusions of previous studies (Salvador, 1987; Mickus, 2009; Stern and Dickinson, 2010) show that the eastern GoM initially underwent a significant amount of strike-slip partitioning as the Yucatan Block separated from North America. This margin presumably then underwent sea floor spreading as a result of both far-field stresses and high-temperature basalt emplacement as the Yucatan Block separated from the Florida Escarpment perpendicular to the transform boundary.

Assuming this interpretation for the nature of rifting in the eastern GoM is correct, it is likely then from the results of this forward modeling that far-field stresses are clearly responsible for the initial separation of the Yucatan Block from the Florida Platform. The thick, complex transition boundary between crust and mantle to the northeast of GUMBO 4 suggests the absence of active, plume driven rifting beneath the Platform, and that the onset of far-field stresses and extensional forces allowed for a void to be filled by high-temperature basaltic magma farther to the southwest, creating the basaltic sheet flows and high velocity upper oceanic crust in the deep water GoM. This evidence supports the findings of previous studies, to include the PLATES reconstruction in Figure 2-13.

Conclusions

1) Moho thickness below the landward end of GUMBO Line 3 is consistently between 1500 and 2000 meters.
2) The thickness beneath GUMBO line 4 is more variable, but covers a wider range of crustal material types. The Moho ranges from ~3500 meters on the landward end of the line to ~1750 meters on the seaward end.
3) The consistent thickness of the relatively narrow Moho beneath GUMBO 3 is indicative of magmatic underplating that produced a sharp transition between crustal and mantle rocks.
4) The thicker Moho on the landward end of GUMBO 4 suggests the absence of magmatic underplating beneath the Florida Platform. This region was most likely not affected by plutonism, and it might be as old as granites and volcanics from the Suwannee Terrane (~552 Ma).
5) The thinning of the Moho as the basement transitions into oceanic crust under GUMBO line 4 is the expected result for this type of margin.

Instrument	Moho Thickness	Model Distance (overlying crust)
OBS 302	1500 m	60 - 75 km (continental)
OBS 305	1750 m	90 - 220 km (transitional)
OBS 309	1500 m	50 - 70 km (continental)
OBS 316	1500 m	65 - 150 km (continental/transitional)
OBS 319	1750 m	135 - 180 km (transitional)
OBS 404	3500 m	65 - 160 km (continental/transitional)
OBS 410	2750 m	150 - 275 km (transitional/oceanic)
OBS 426 (Landward)	2000 m	180 - 275 km (transitional/oceanic)
OBS 426 (Seaward)	1750 m	310 - 335 km (oceanic)

Table 3-1: Moho Thicknesses

Determined Moho thicknesses for each instrument selected for GUMBO lines 3 and 4 along with overlying crustal types.

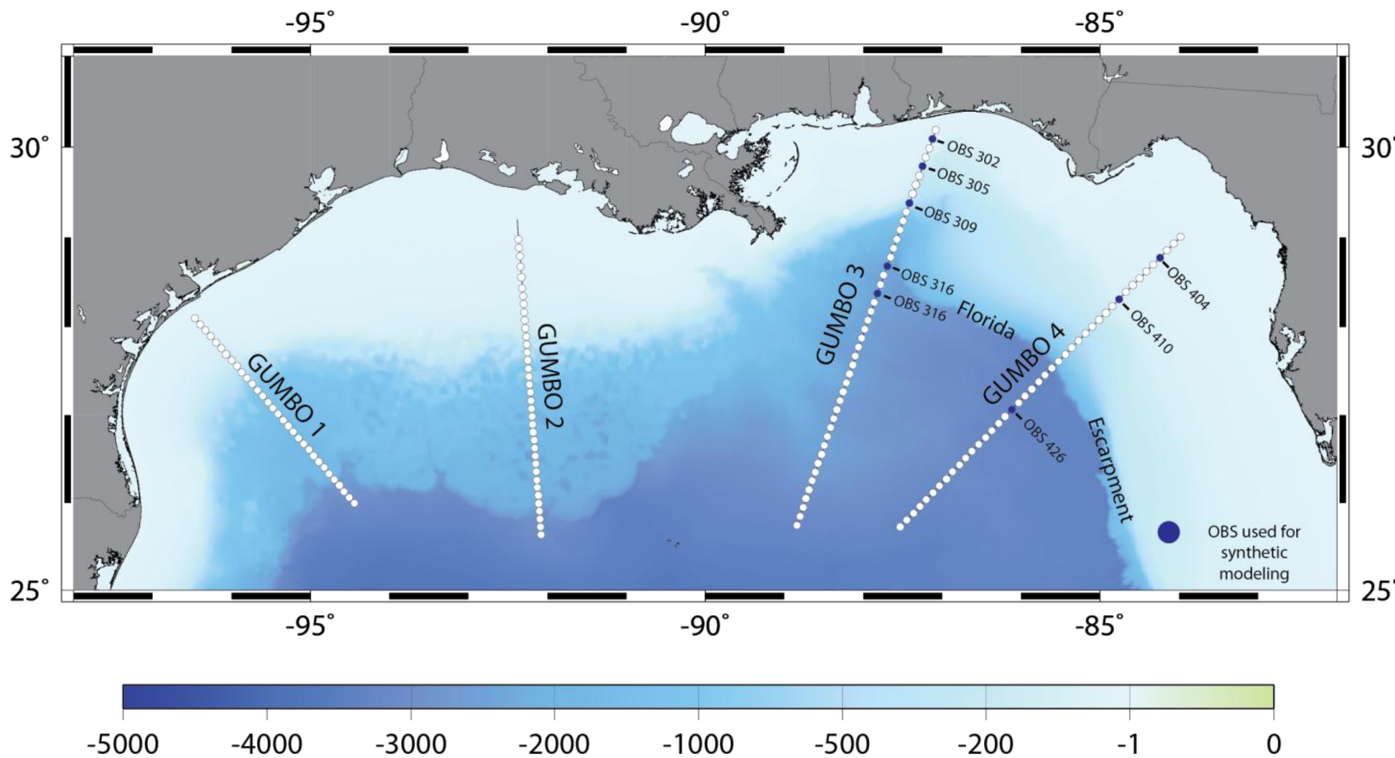

Figure 3-1: Study Area, Forward Modeling

Study area for investigation of the nature of the Moho. Blue circles represent locations of OBSs used for synthetic modeling.

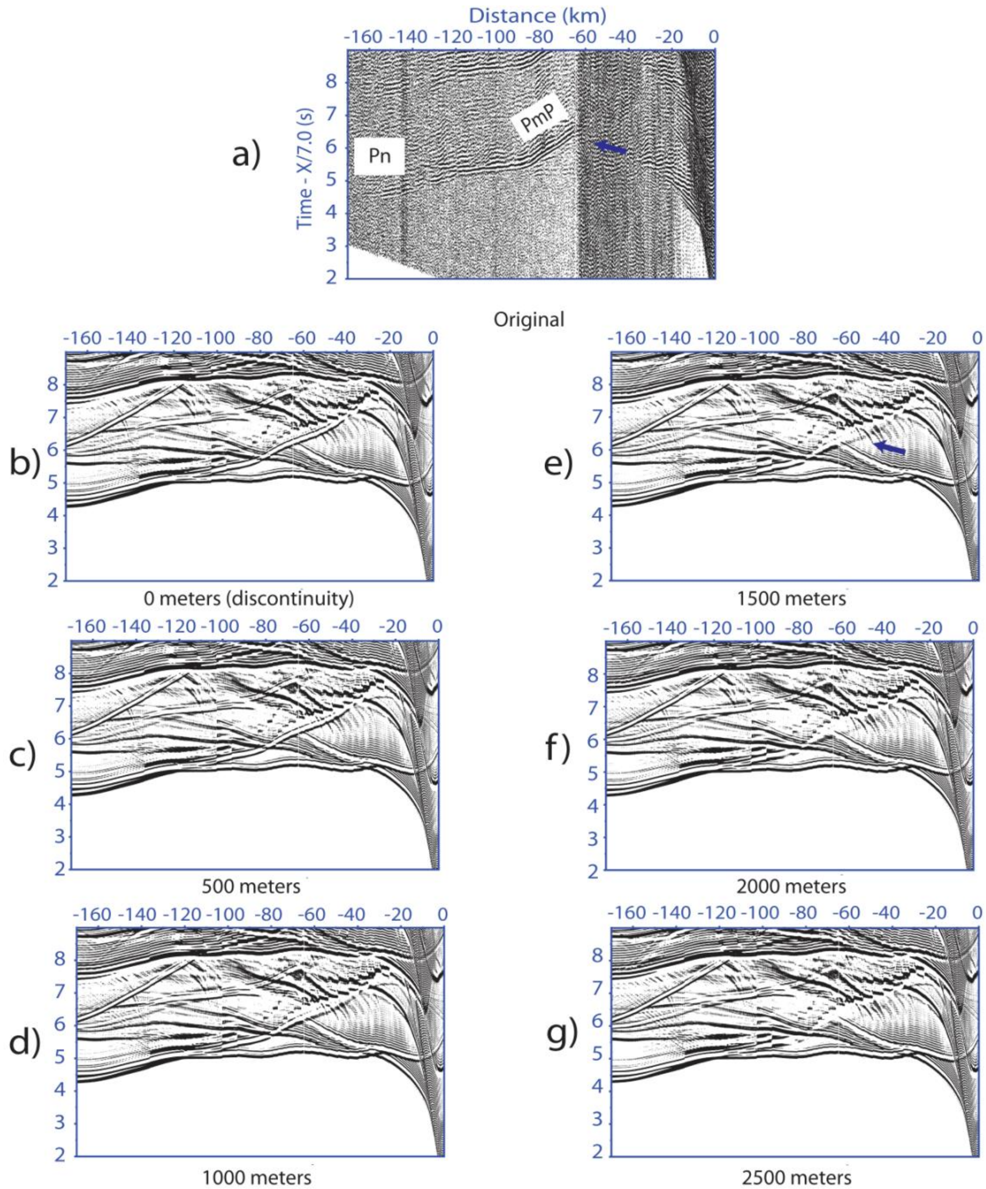

Figure 3-2: OBS 316 Synthetic Models

OBS 316 original receiver gather (top) with Pn and PmP arrivals labeled. Synthetic models show the difference in amplitudes for a 0 to 2500 meter thick transition zone. Blue arrow shows the location of the onset of the PmP arrival in the original (6 seconds, 60 km offset) and in the 1500 meter thickness synthetic model. The data have been passed through a Butterworth filter with a low cut of 3 Hz and a high cut of 15 Hz. Record sections are plotted with a reduction velocity of 7 km/s. Amplitudes have been range scaled by a factor of $R^{1.0}$, where R is the distance of the shot from the receiver.

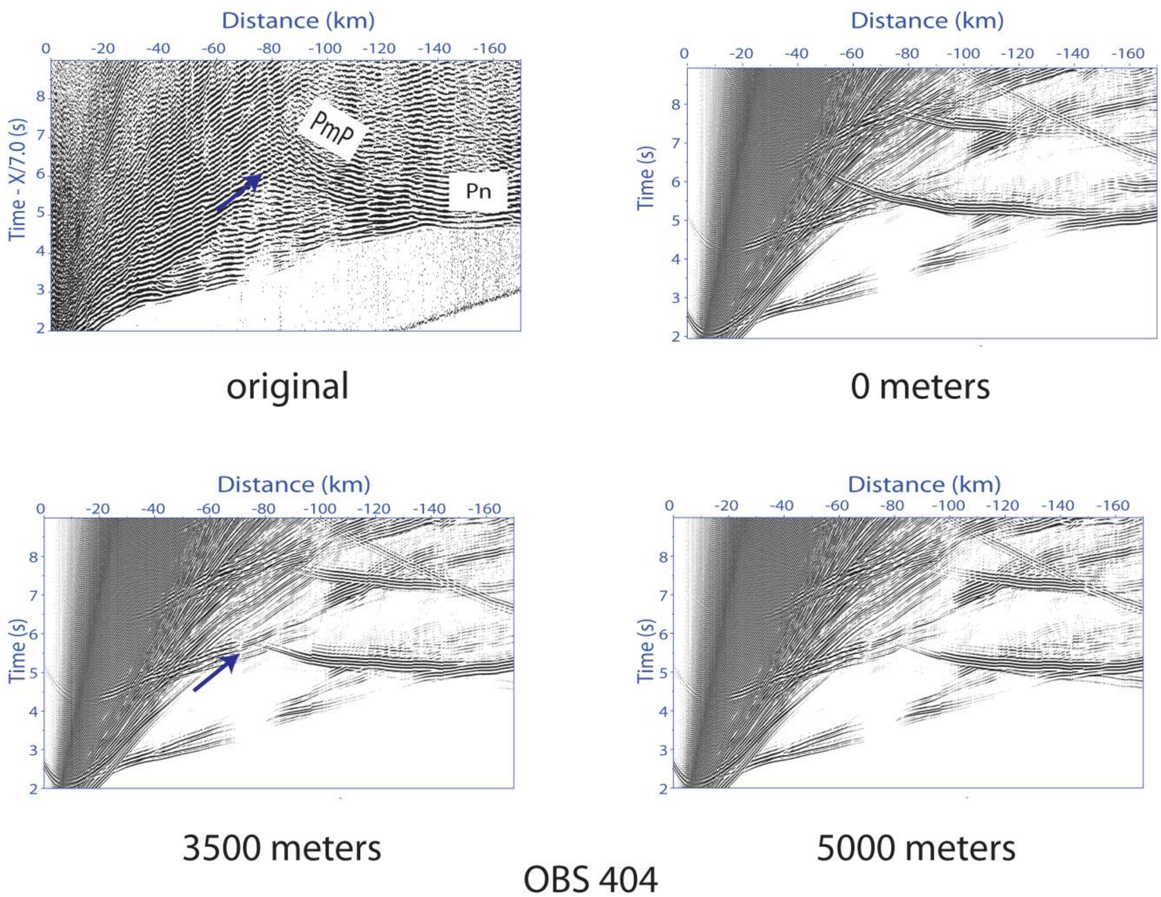

Figure 3-3: OBS 404 Synthetic Models

OBS 404 original receiver gather with Pn and PmP arrivals labeled. Synthetic models show the difference in PmP and Pn amplitudes with variations from a 0 to 5000 meter thick transition zone. Blue arrow marks the onset of the PmP arrival (6 seconds ~80 km offset) in original and at synthetic 3500 meter thickness. The data have been passed through a Butterworth filter with a low cut of 3 Hz and a high cut of 15 Hz. Record sections are plotted with a reduction velocity of 7 km/s. Amplitudes have been range scaled by a factor of $R^{1.0}$, where R is the distance from the shot from the receiver.

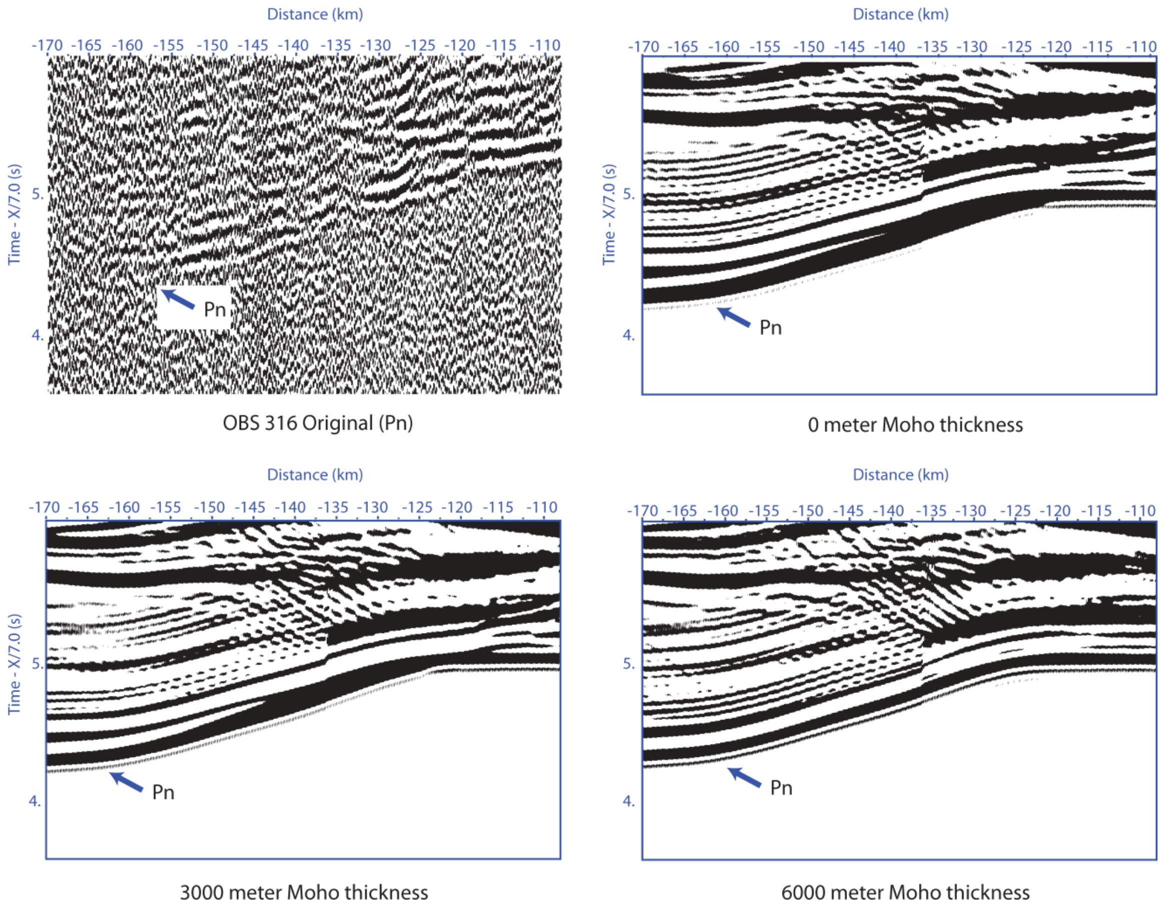

Figure 3-4: OBS 316 Pn Arrivals

Detail of the Pn arrival for OBS 316. Synthetic models indicate a Moho 0, 3000, and 6000 meters in thickness. Pn amplitudes decrease at near offsets and increase at far offsets with increasing crust-mantle transition zone thickness.

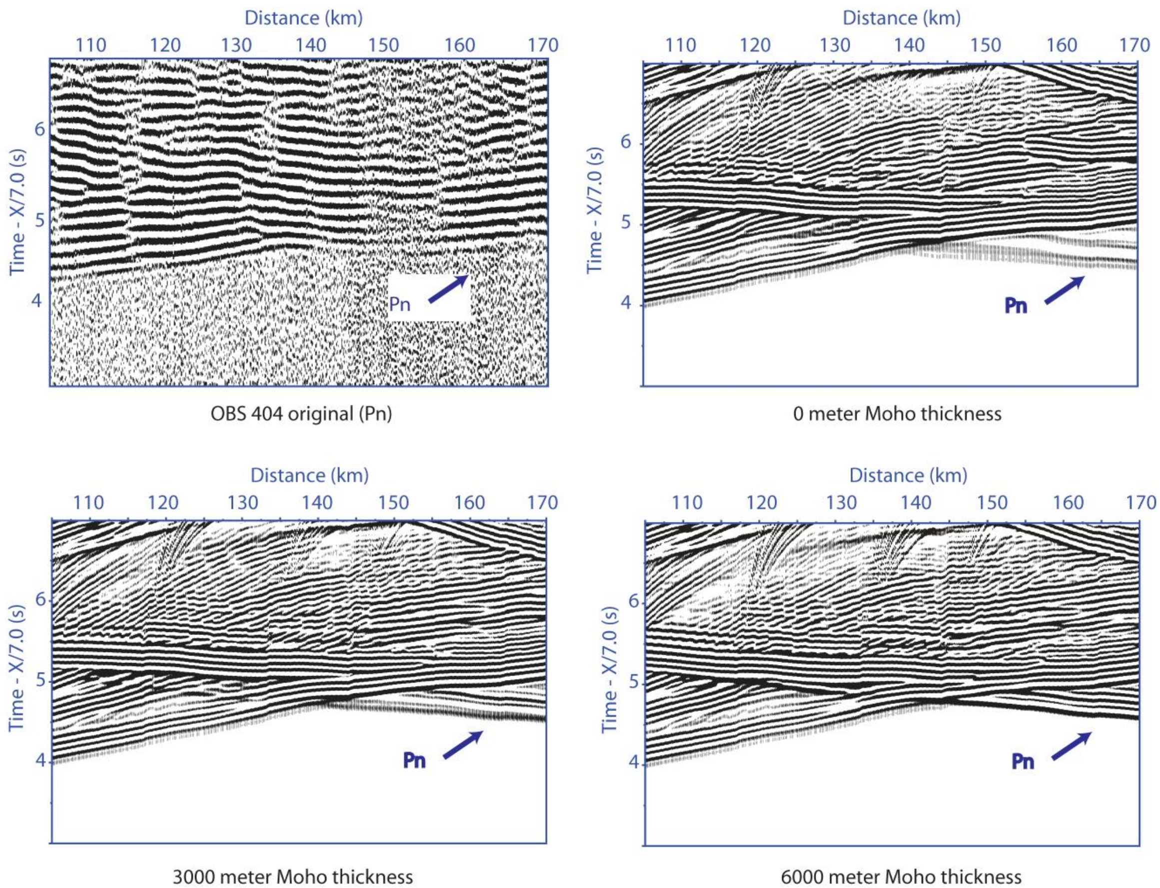

Figure 3-5: OBS 404 Pn Arrivals

Detail of the Pn arrival for OBS 404. Synthetic models indicate a Moho 0, 2500, and 5000 meters in thickness. Pn amplitudes increase with increasing crust-mantle transition zone thickness.

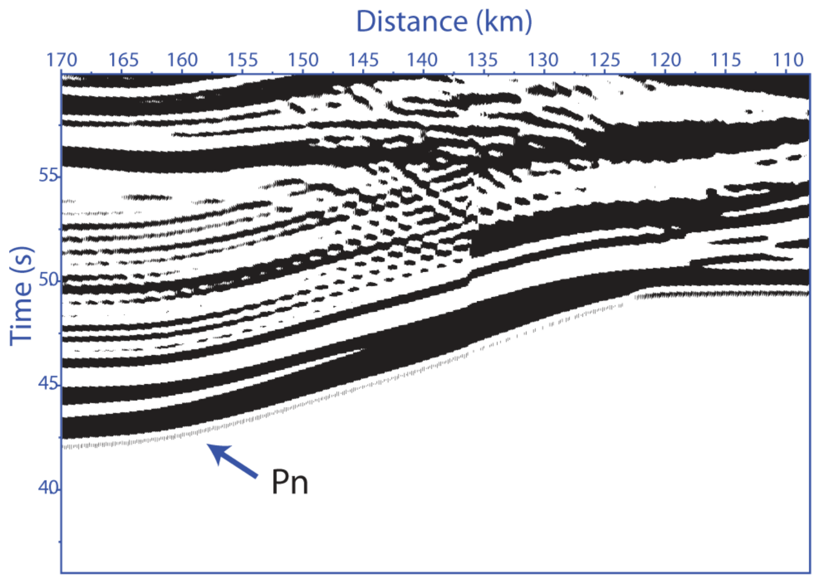

OBS 316 (-0.001km/s/km Mantle Gradient)

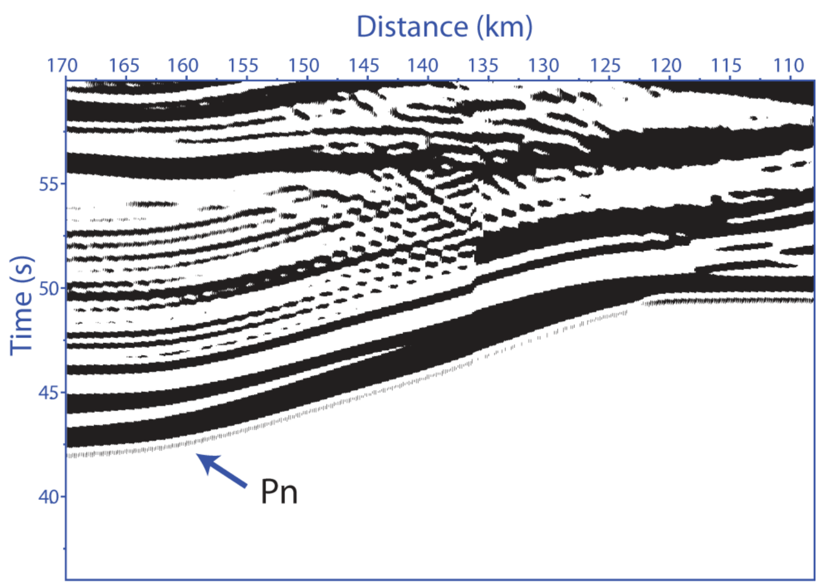

OBS 316 (0.004 km/s/km Mantle Gradient)

Figure 3-6: OBS 316 Effects of Mantle Gradient Variation

Effects of mantle gradient variance on Pn amplitudes. The two extremes tested, (-0.001 and 0.004) display a negligible difference in the appearance of the Pn arrival.

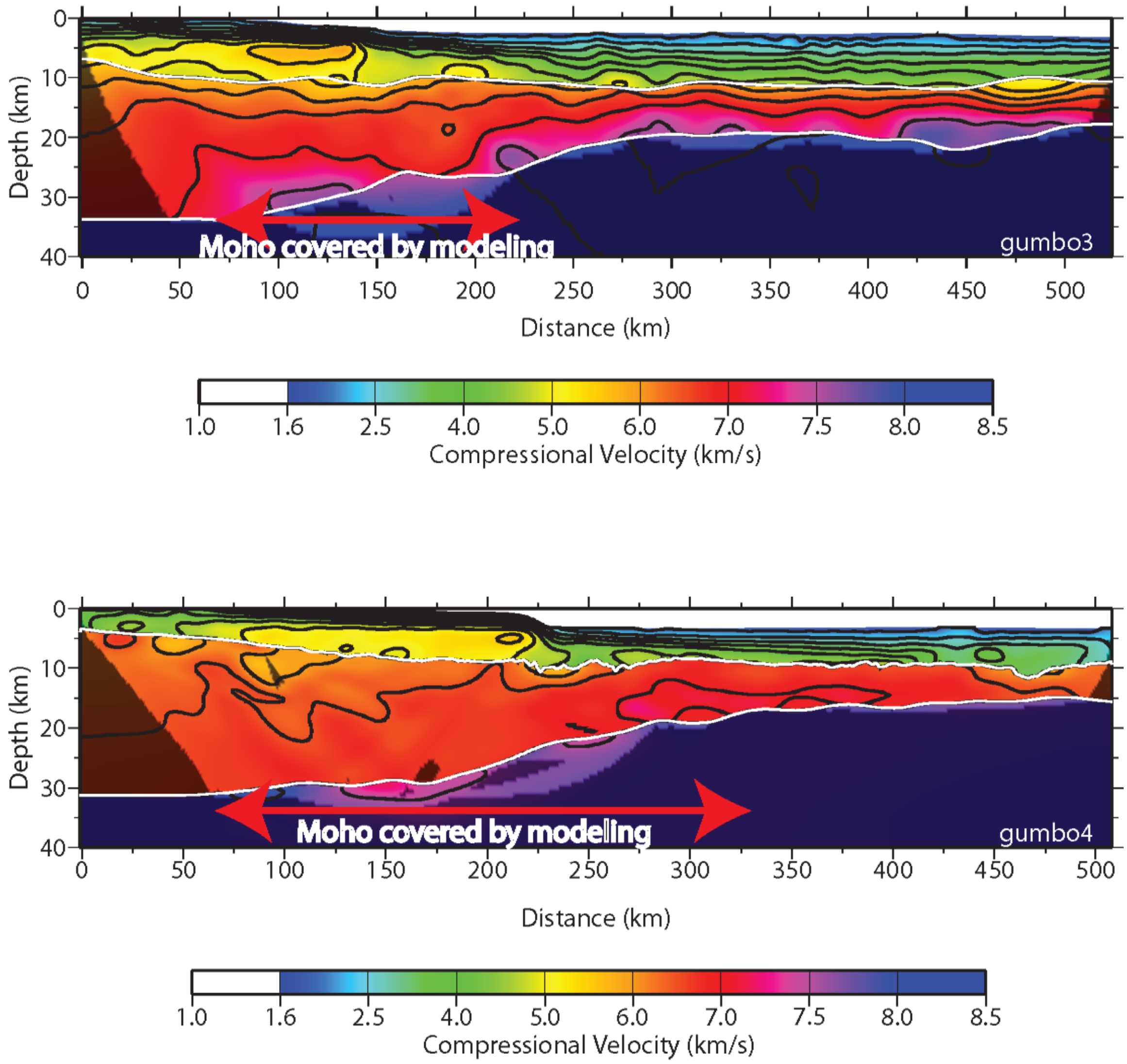

Figure 3-7: GUMBO 3 and 4 P-wave Velocity Models

P-wave velocity models for GUMBO lines 3 and 4. Red arrow indicates the lateral area covered by synthetic modeling of the Moho. White lines are boundaries between the sediment and crustal layers and between the crust and upper mantle layers.

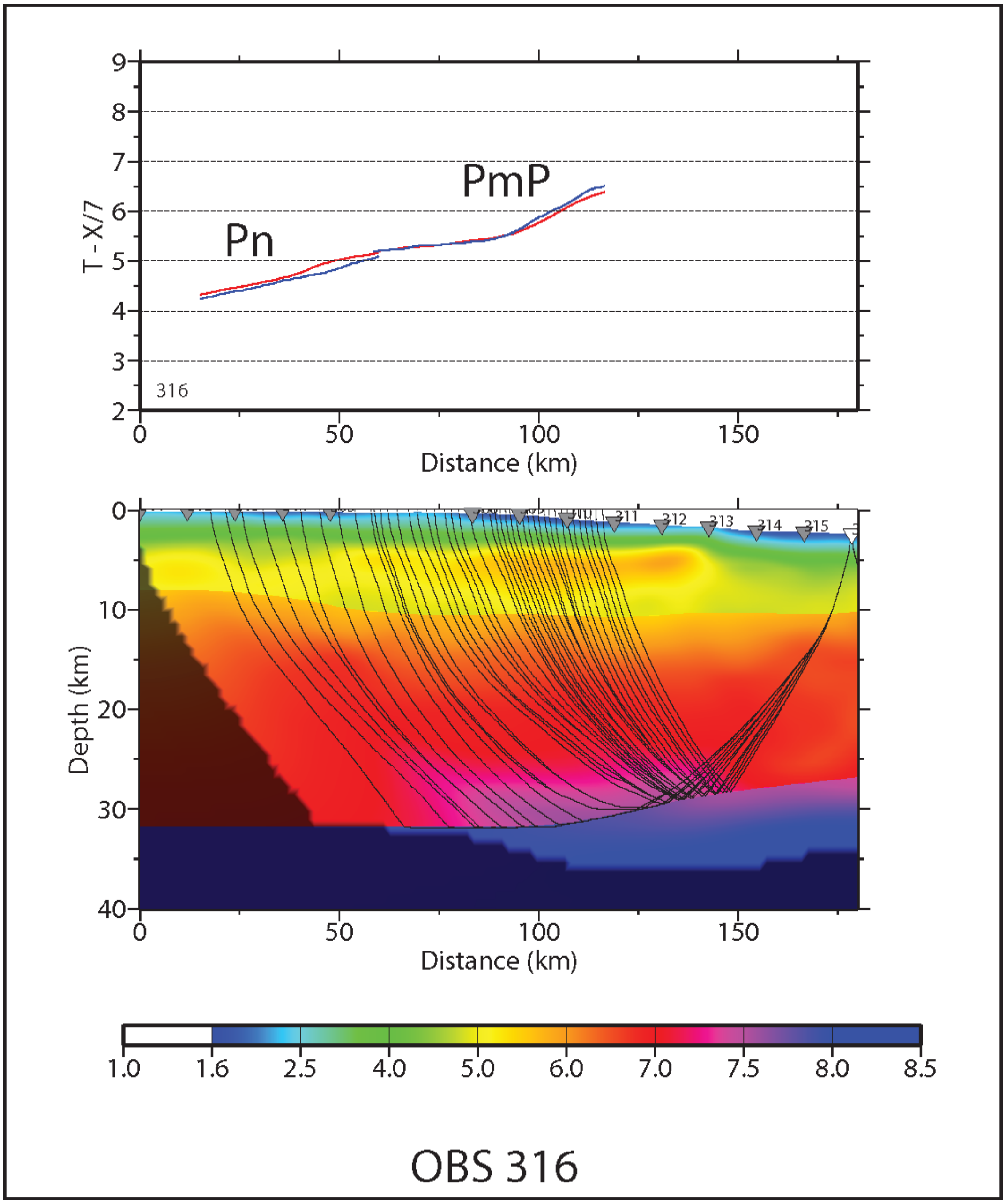

Figure 3-8: OBS 316 Ray Tracing Diagram

Ray tracing diagram for OBS 316. Pn and PmP arrivals are labeled. This instrument and the ray paths associated with it cover a section of Moho overlain by continental and transitional crust

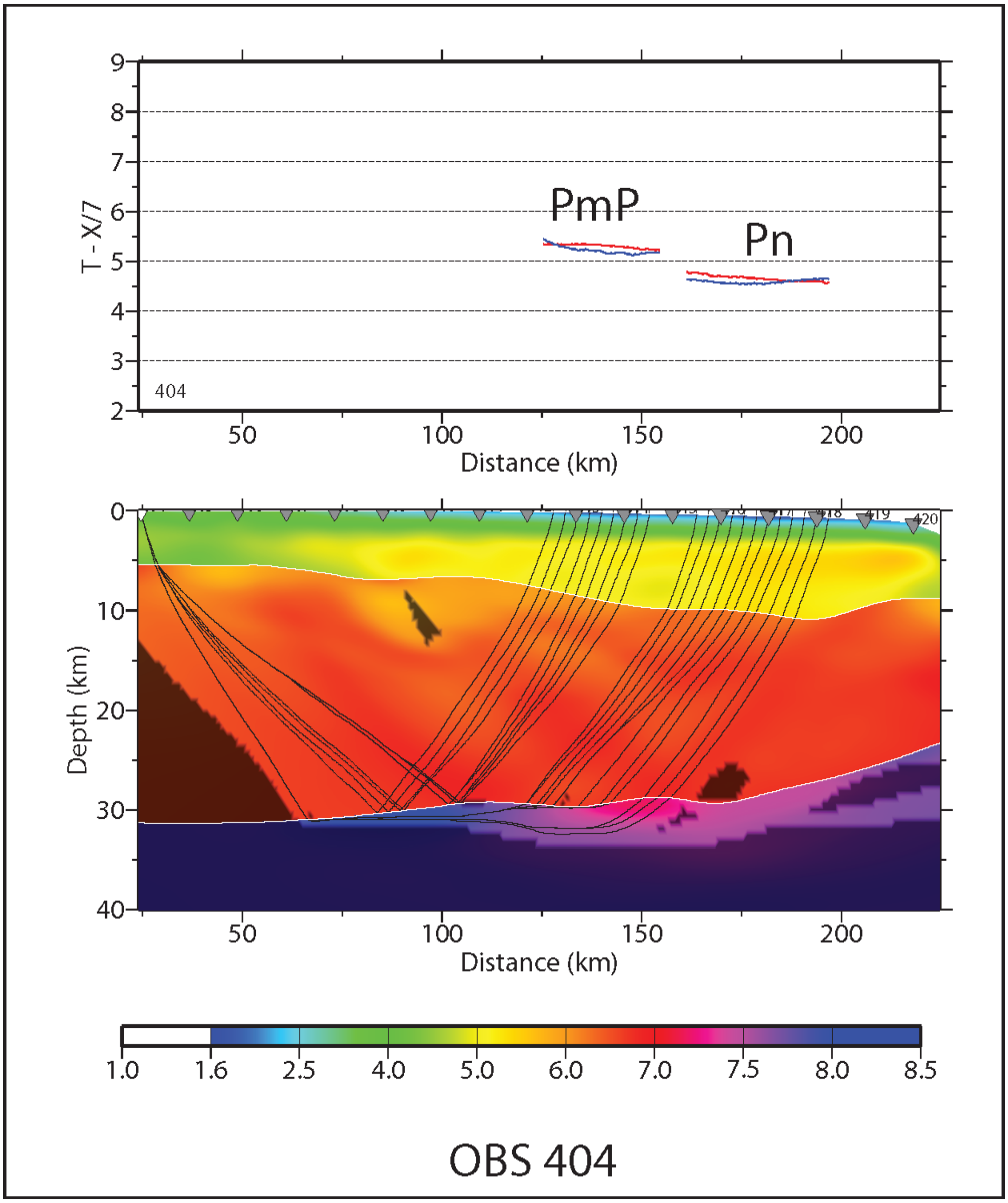

Figure 3-9: OBS 404 Ray Tracing Diagram

Ray tracing diagram for OBS 404. Pn and PmP arrivals are labeled. This instrument and the ray paths associated with it cover a section of Moho overlain by continental and transitional crust

Appendix A

The following figures display the receiver gathers for the ten remaining Ocean Bottom Seismometers used to pick shear wave arrivals from GUMBO line 4. Sg arrivals (shear-wave crustal refractions) are shown as red lines, and SmS arrivals (shear-wave Moho reflections) are shown as blue lines in both the zoomed in and zoomed out views of the receiver gather.

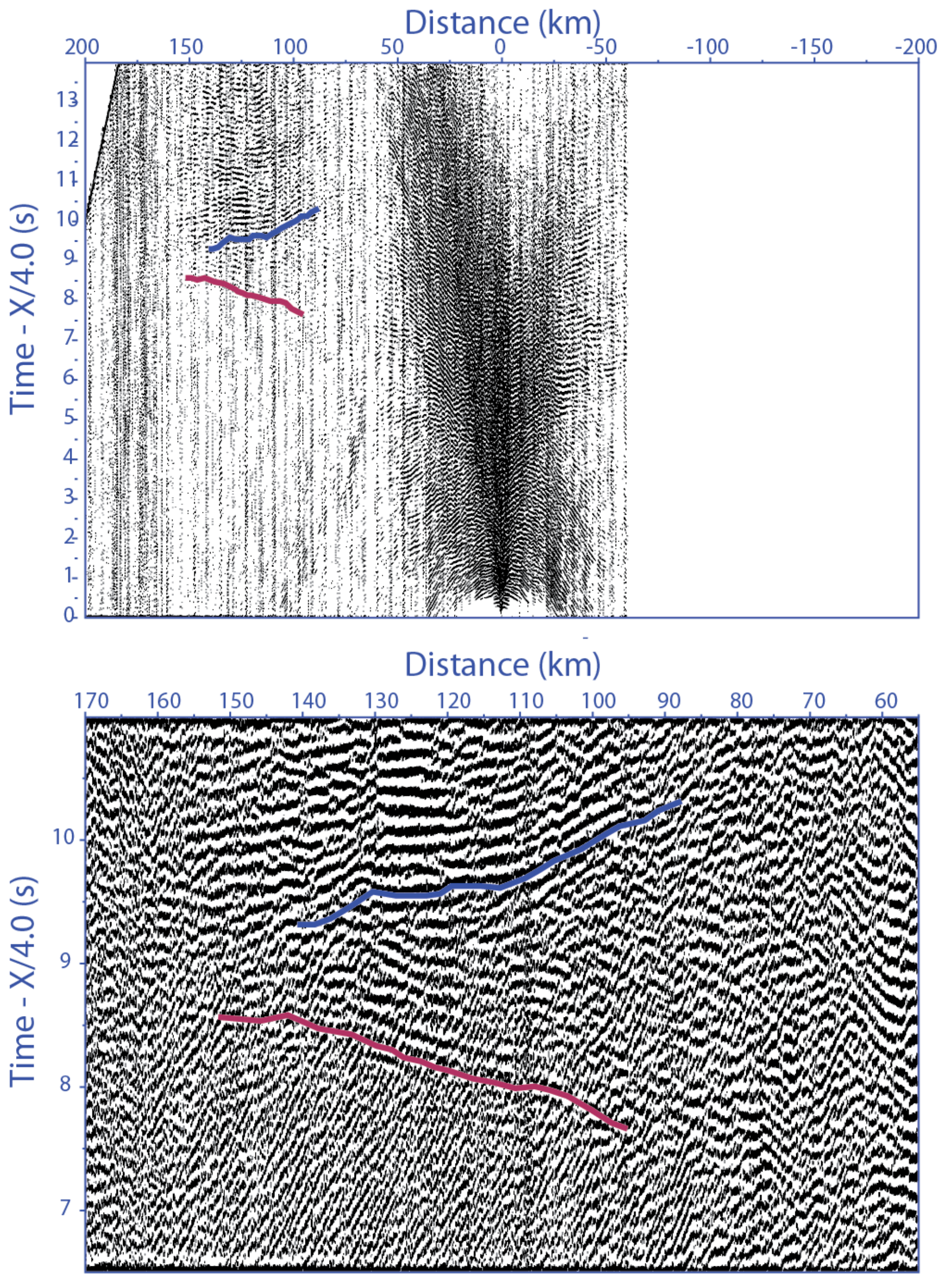

Figure A-1: OBS 407 shear-wave arrivals

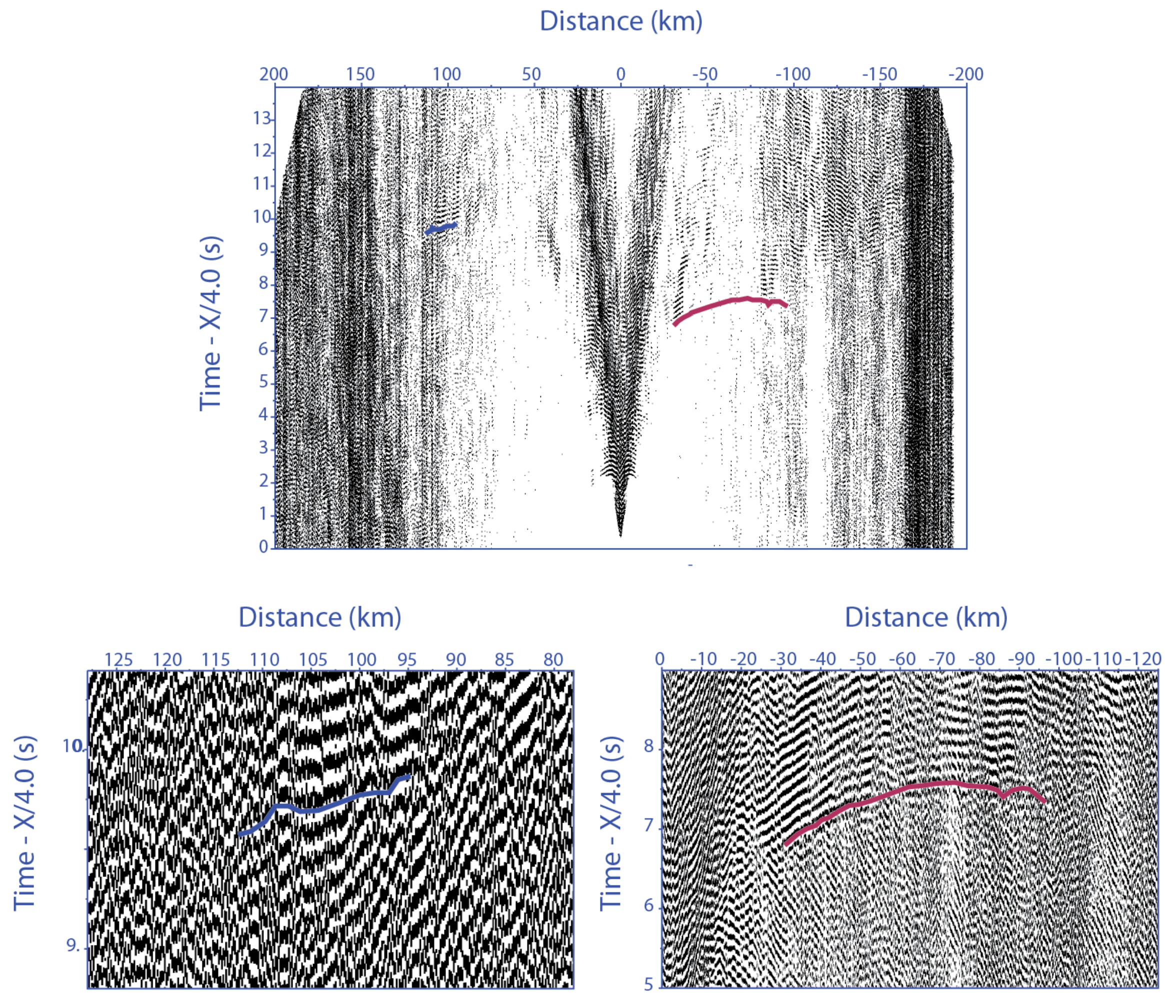

Figure A-2: OBS 418 shear-wave arrivals

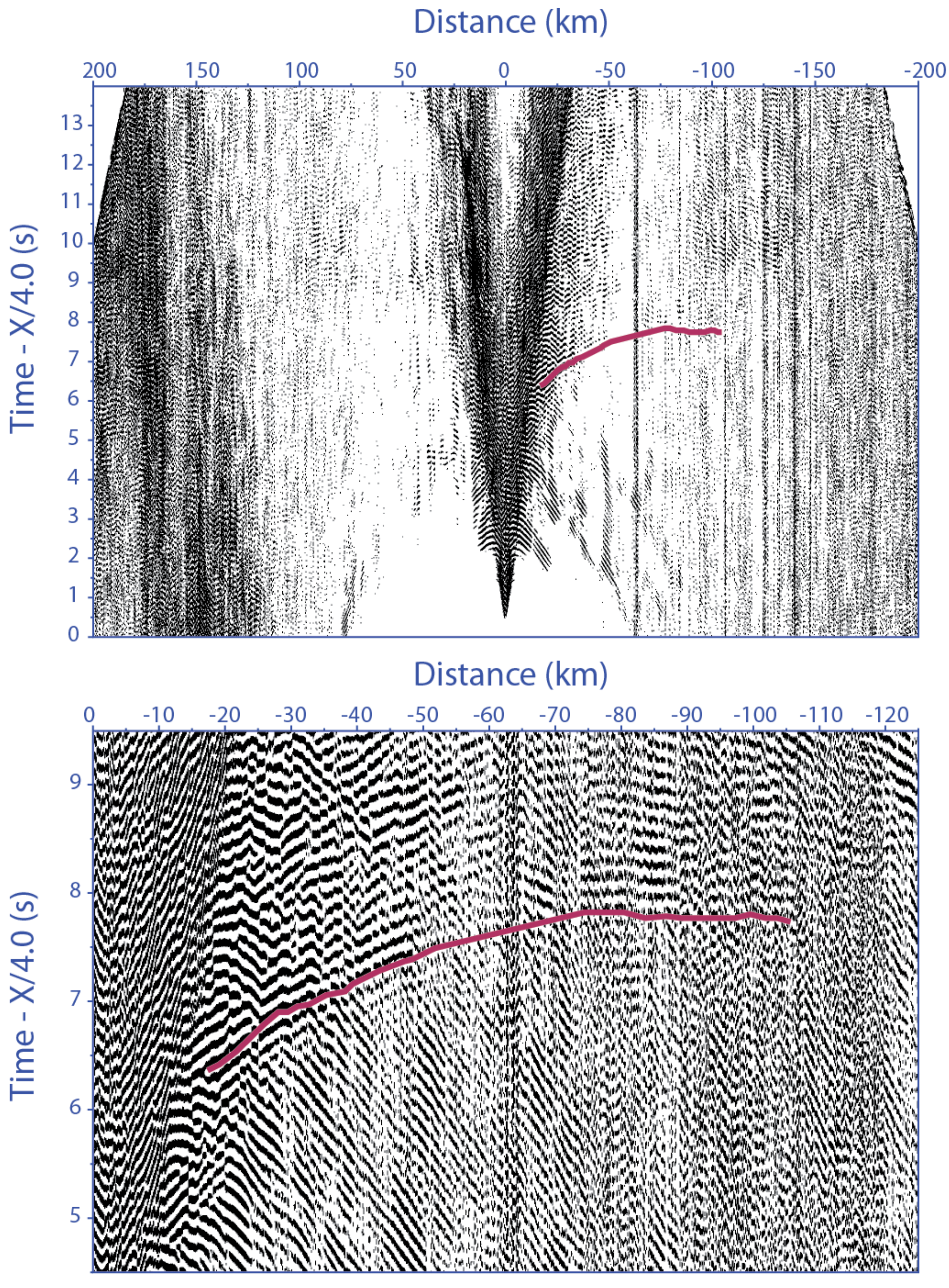

Figure A-3: OBS 419 shear-wave arrival

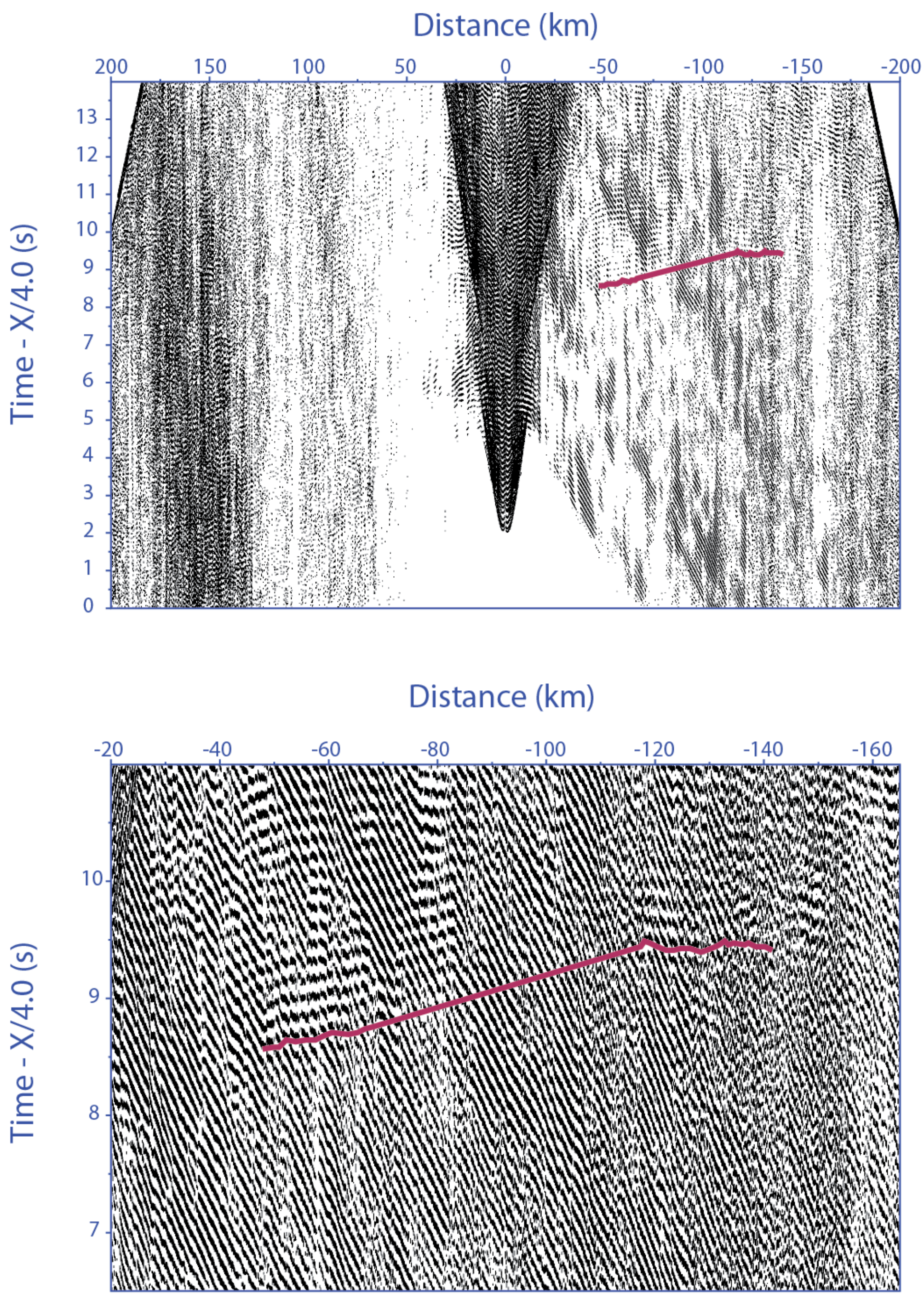

Figure A-4: OBS 422 shear-wave arrival

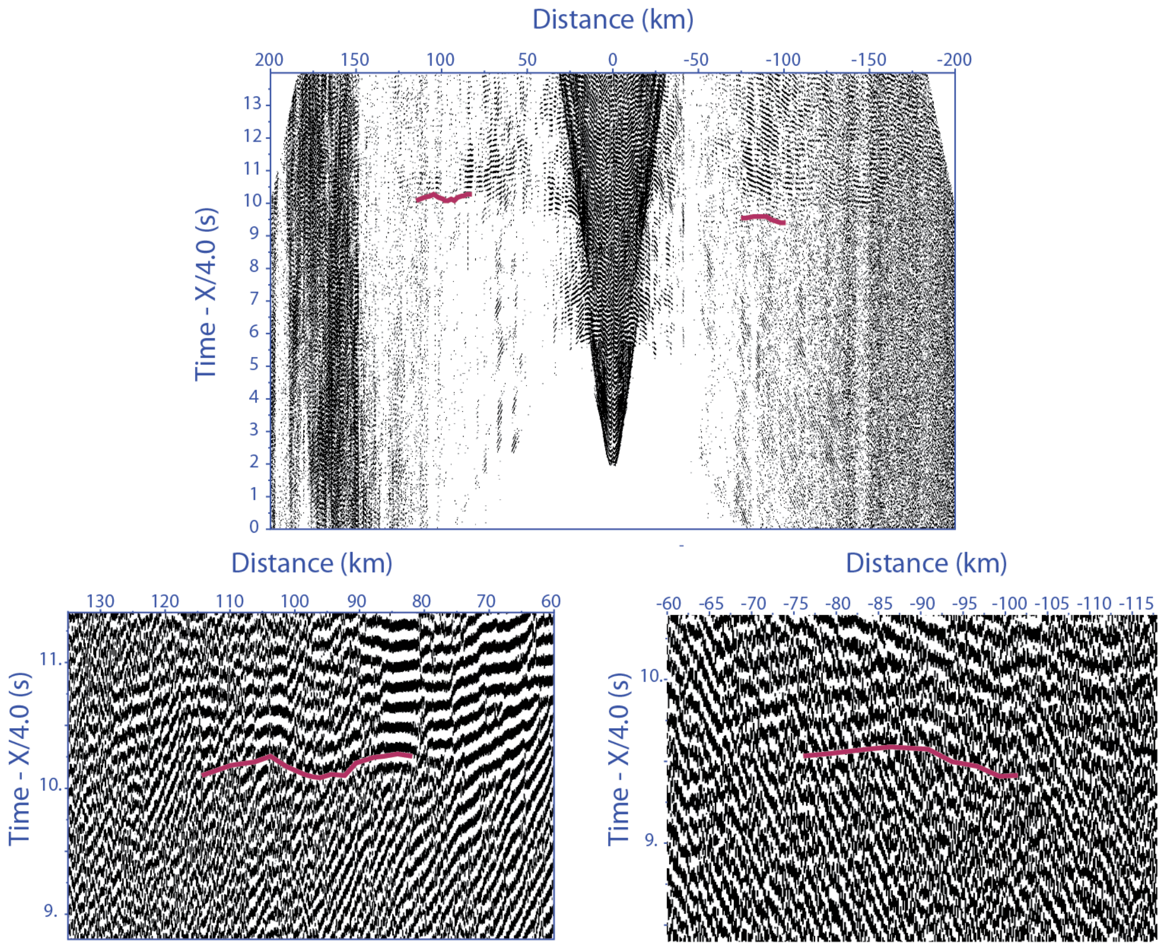

Figure A-5: OBS 424 shear-wave arrivals

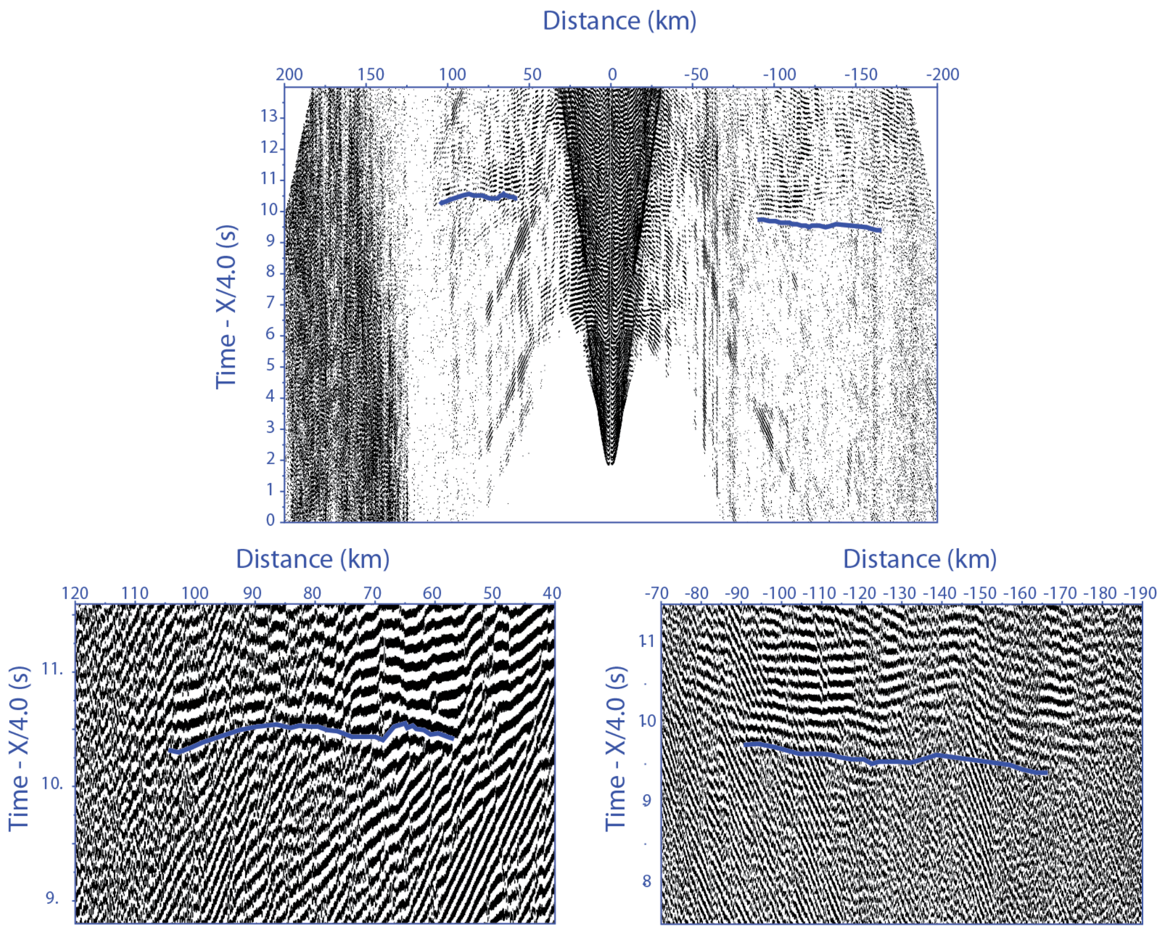

Figure A-6: OBS 426 shear-wave arrivals

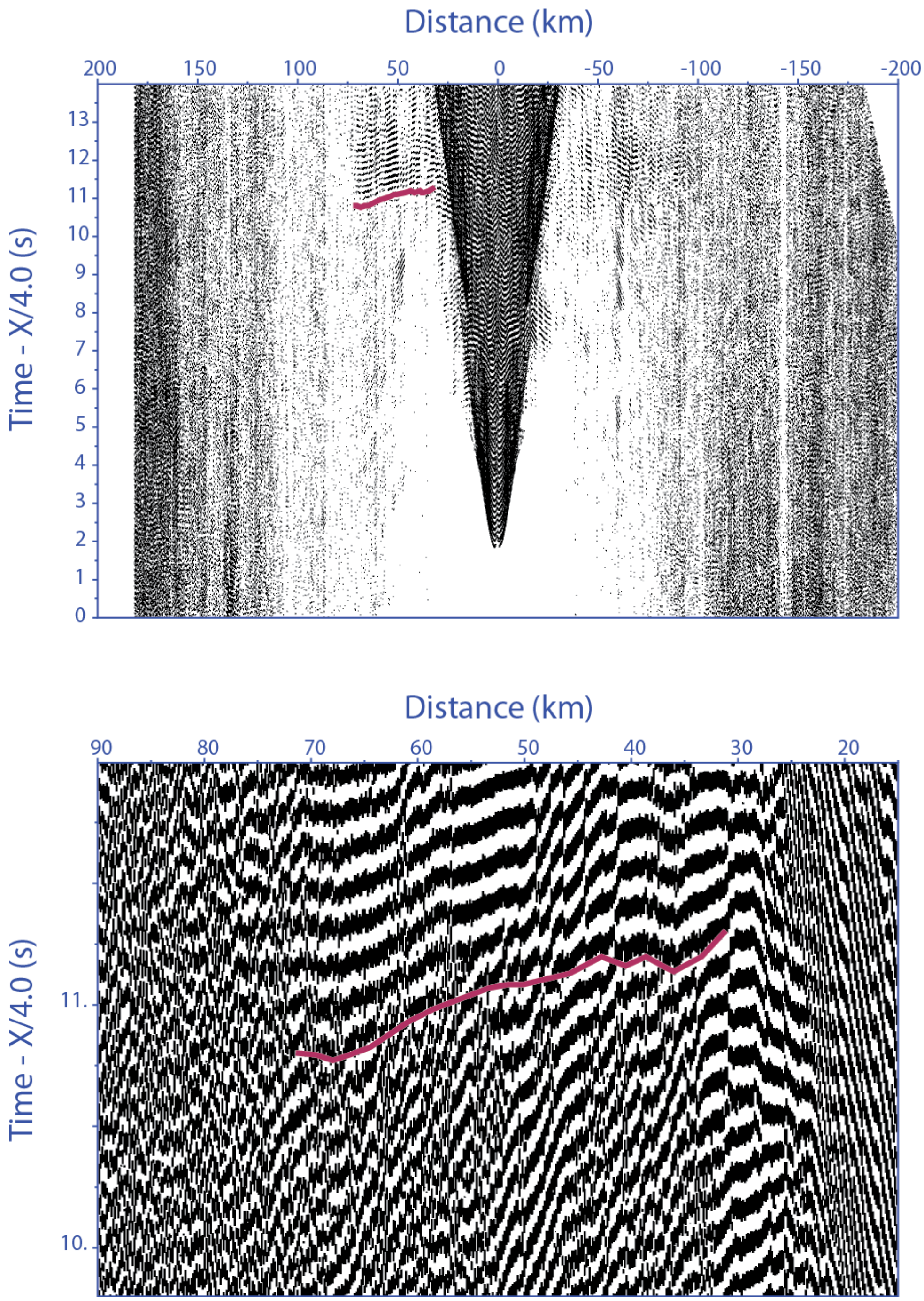

Figure A-7: OBS 429 shear-wave arrival

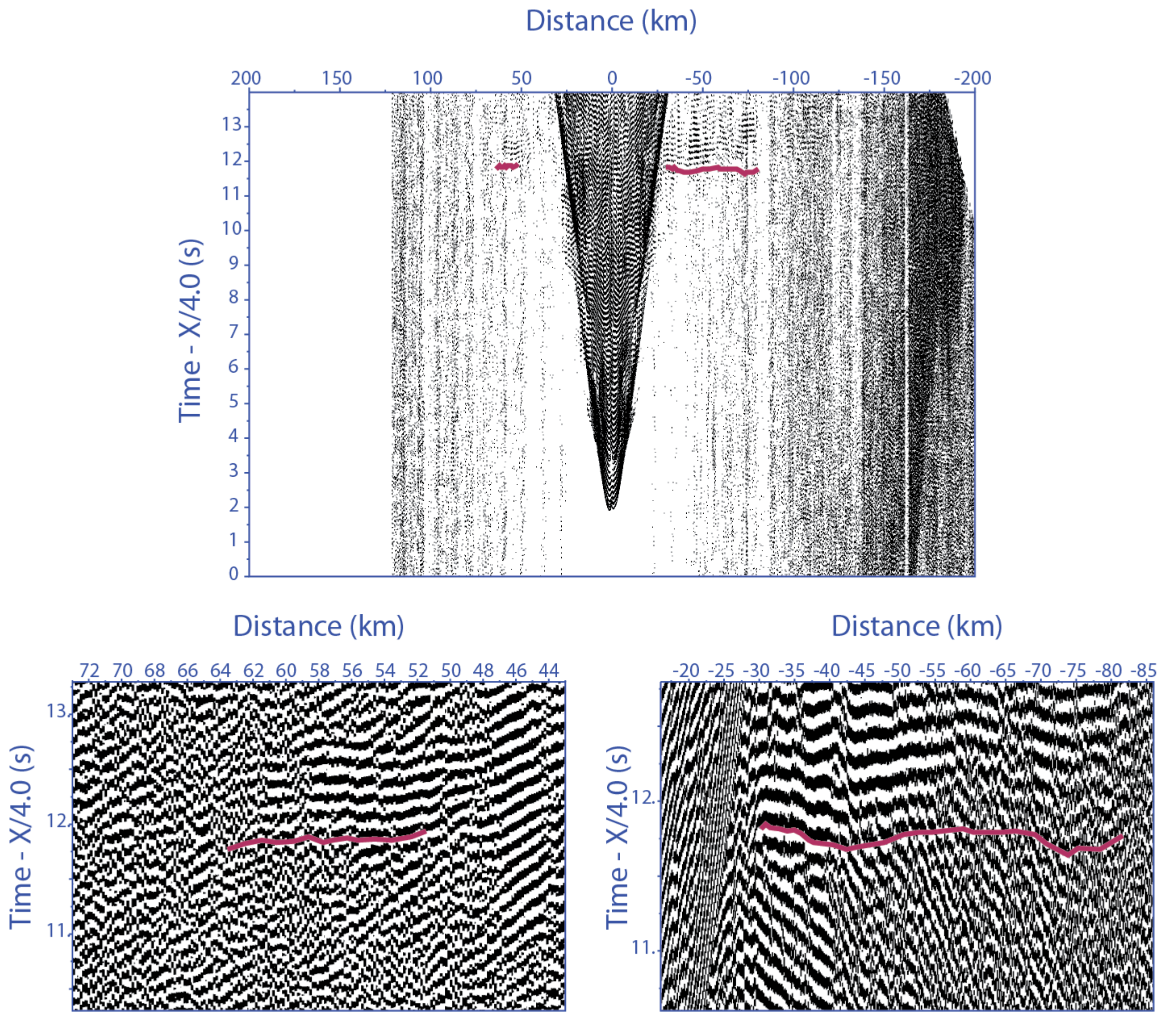

Figure A-8: OBS 434 shear-wave arrivals

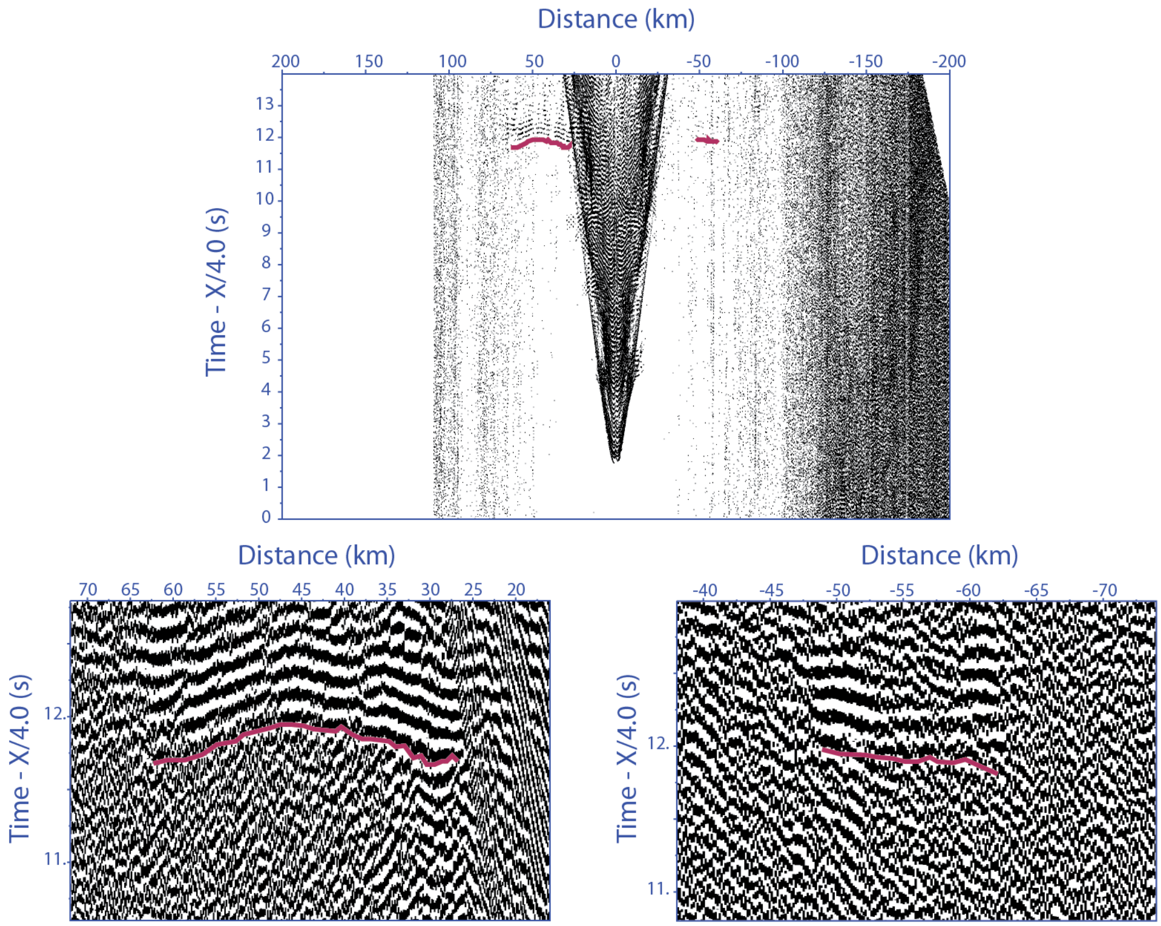

Figure A-9: OBS 435 shear-wave arrivals

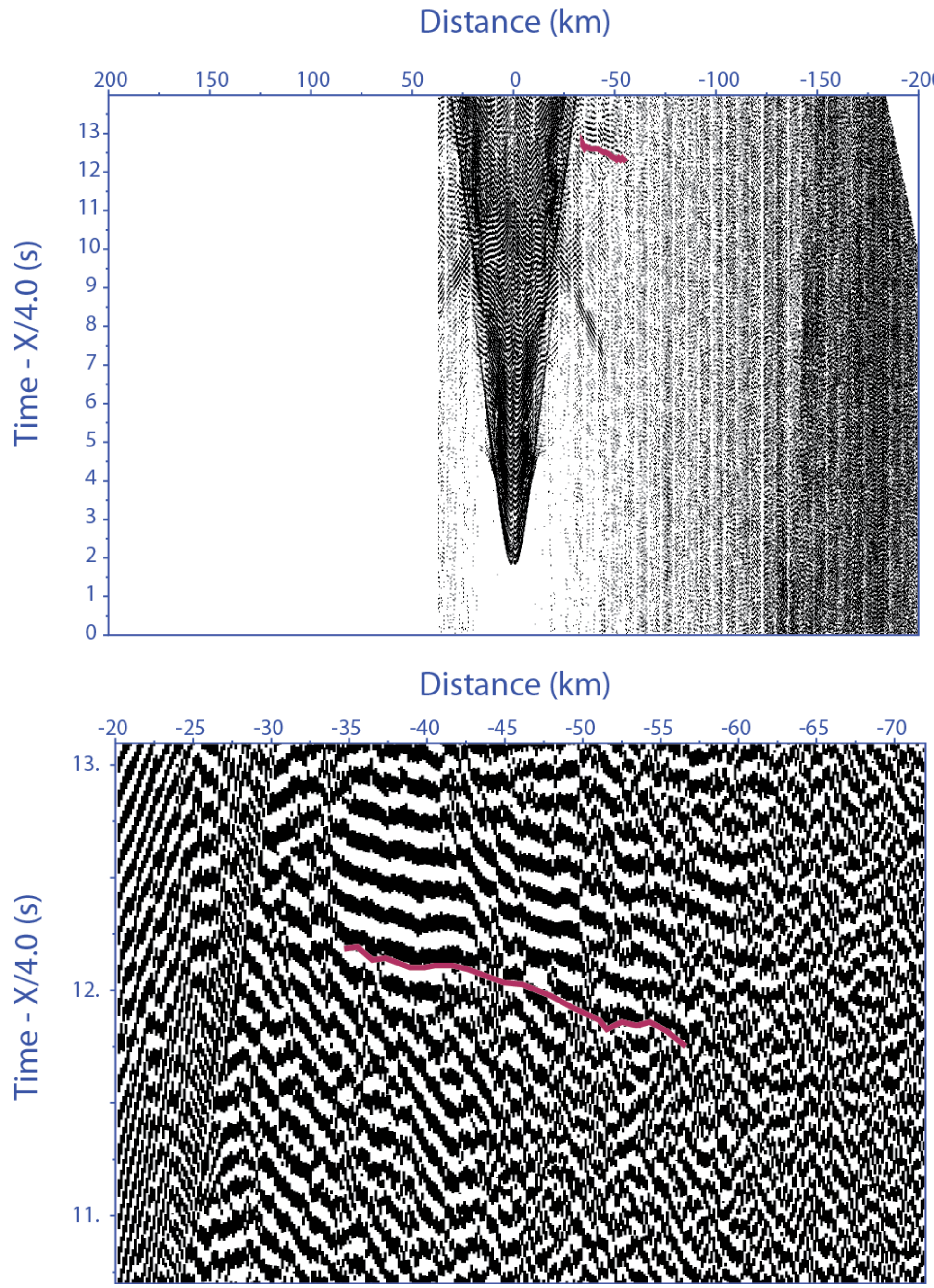

Figure A-10: OBS 441 shear-wave arrivals

Appendix B

The following figures display a range of synthetic receiver gathers for the remaining six Ocean Bottom Seismometers used to investigate the nature of the Moho beneath GUMBO Lines 3 and 4. Six different thicknesses are shown for each instrument. Table 3-1 shows the determined thicknesses for each instrument. The distance from the receiver and the amplitudes for the onset of PmP arrivals (compressional-wave) are what are used to determine the thickness of the crust-mantle transition.

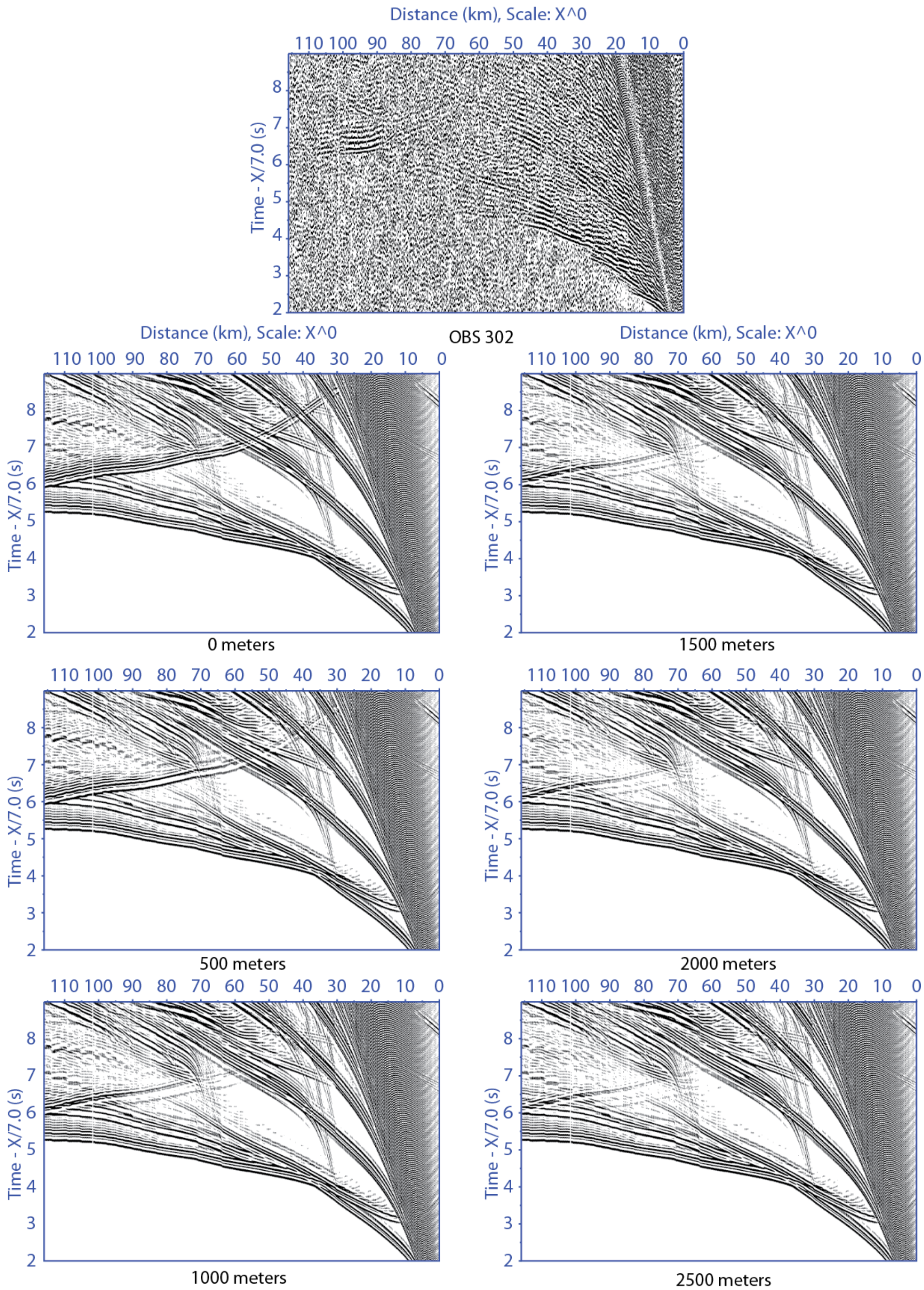

Figure B-1: OBS 302 Synthetic Models

Synthetic models from 0 to 2500 meter crust-mantle transition

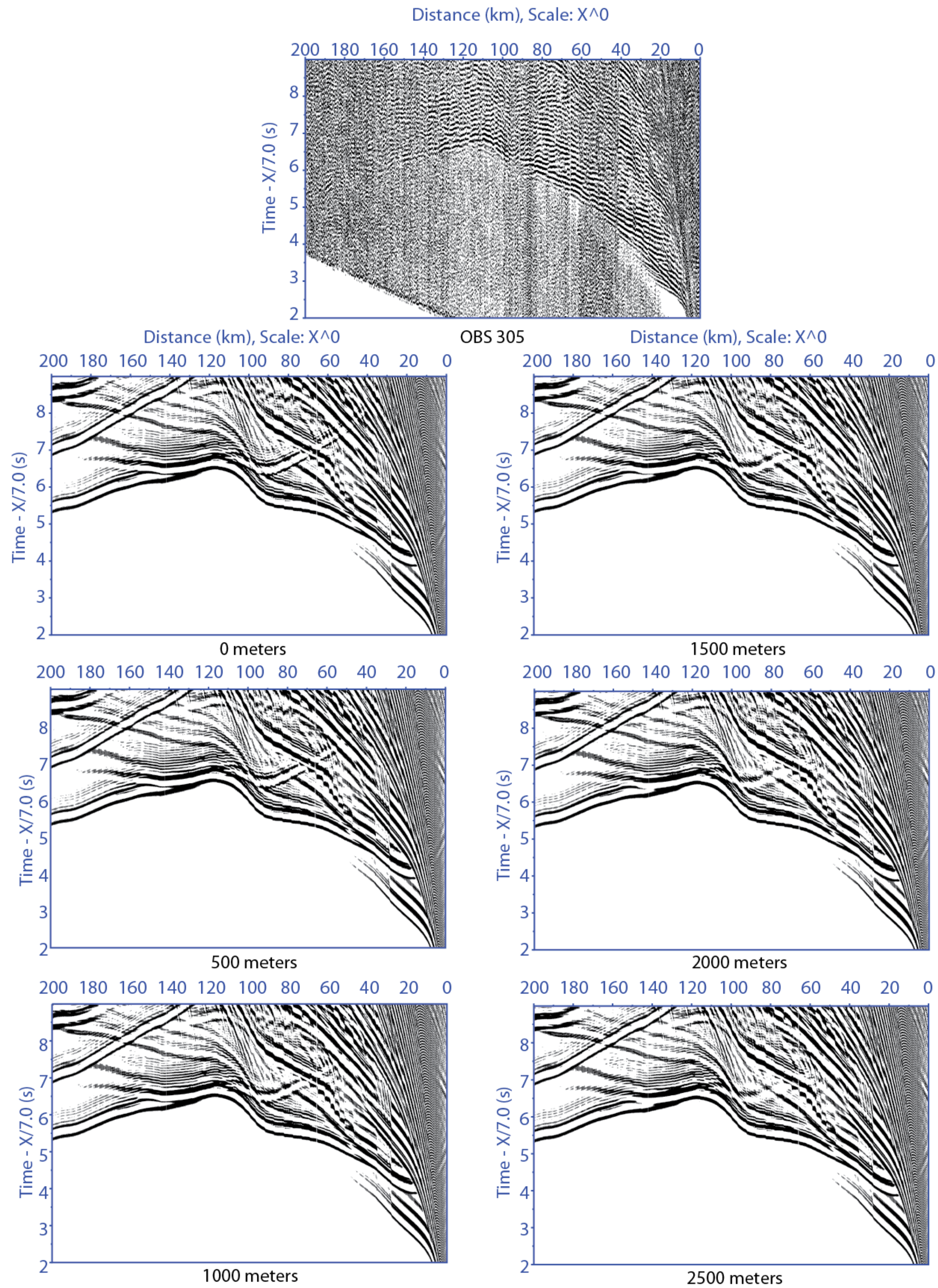

Figure B-2: OBS 305 Synthetic Models

Synthetic models from 0 to 2500 meter crust-mantle transition thickness

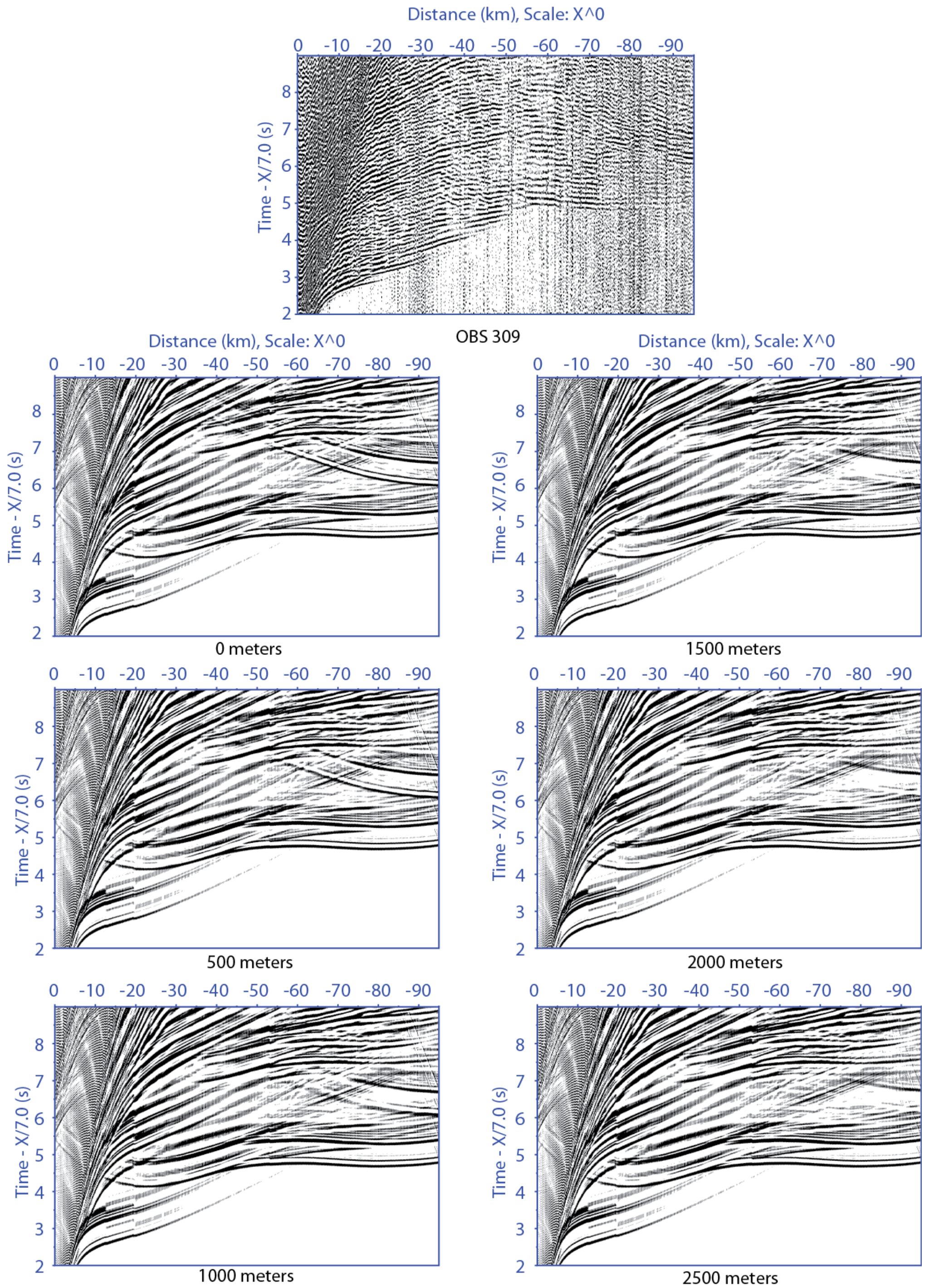

Figure B-3: OBS 309 Synthetic Models

Synthetic models from 0 to 2500 meter crust-mantle transition thickness

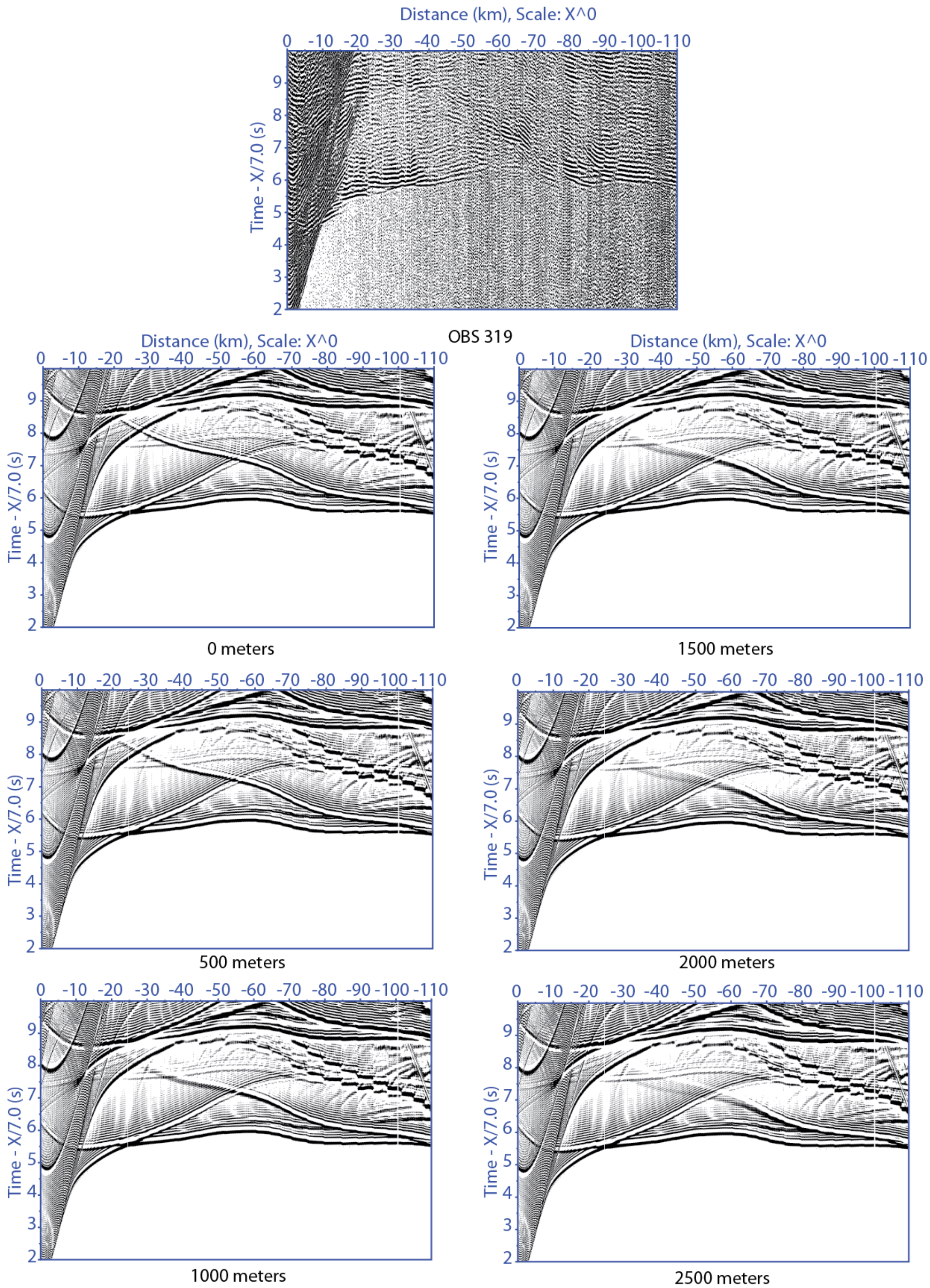

Figure B-4: OBS 319 Synthetic Models

Synthetic models from 0 to 2500 meter crust-mantle transition thickness

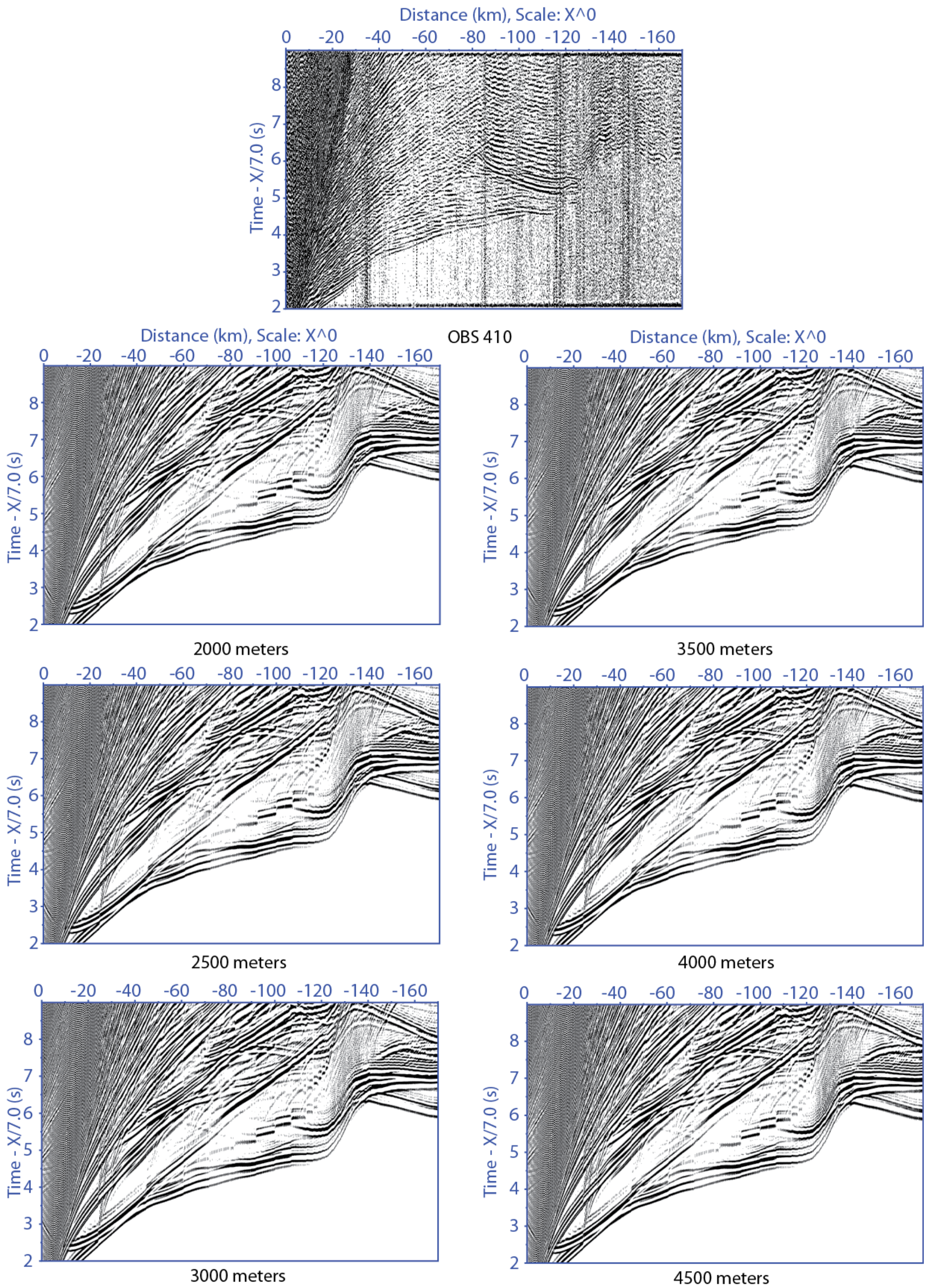

Figure B-5: OBS 410 Synthetic Models

Synthetic models from 2000 to 4500 meter crust-mantle transition thickness

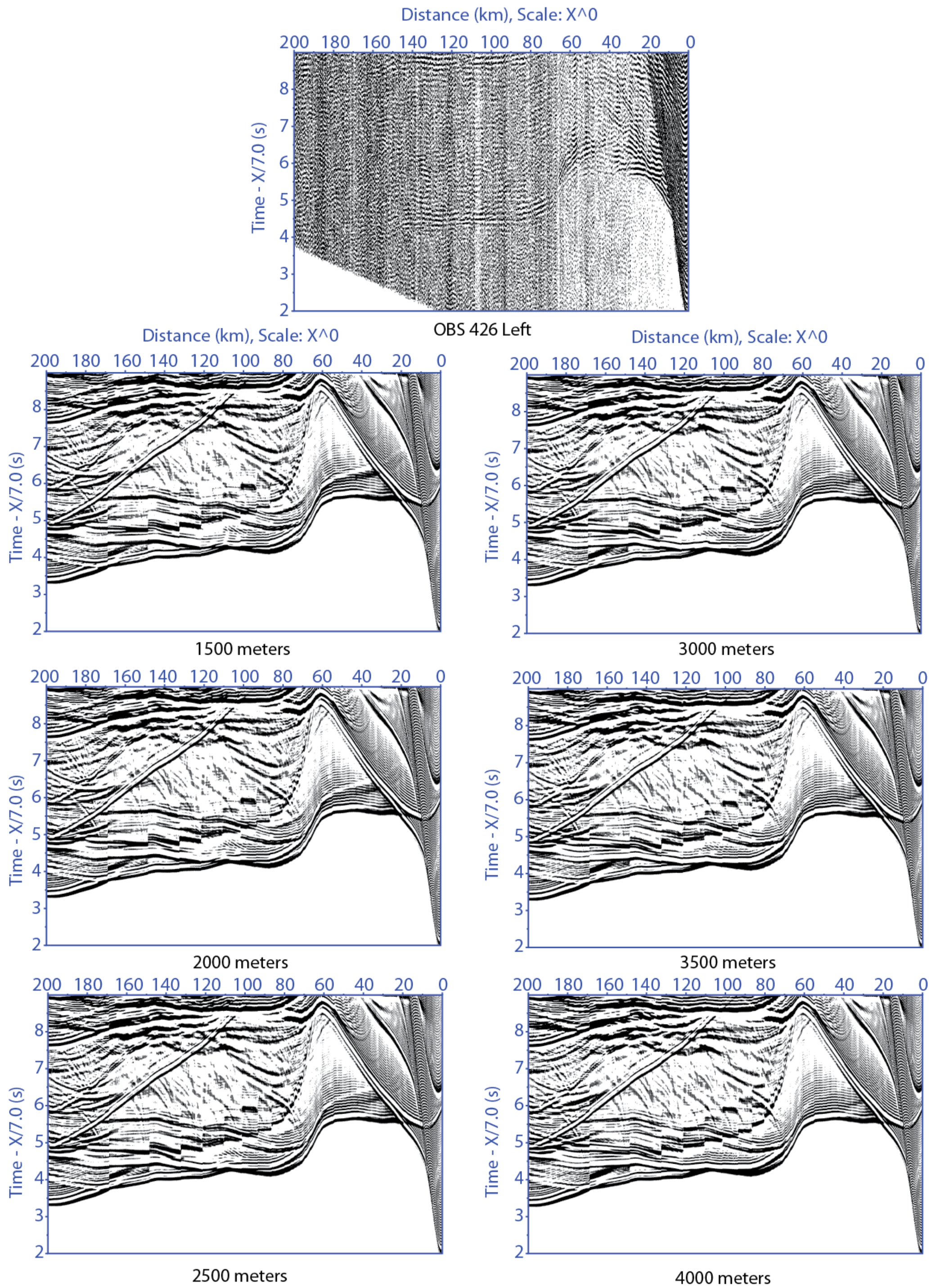

Figure B-6: OBS 426 (left offset) Synthetic Models

Synthetic models for 1500 to 4000 meter crust-mantle transition

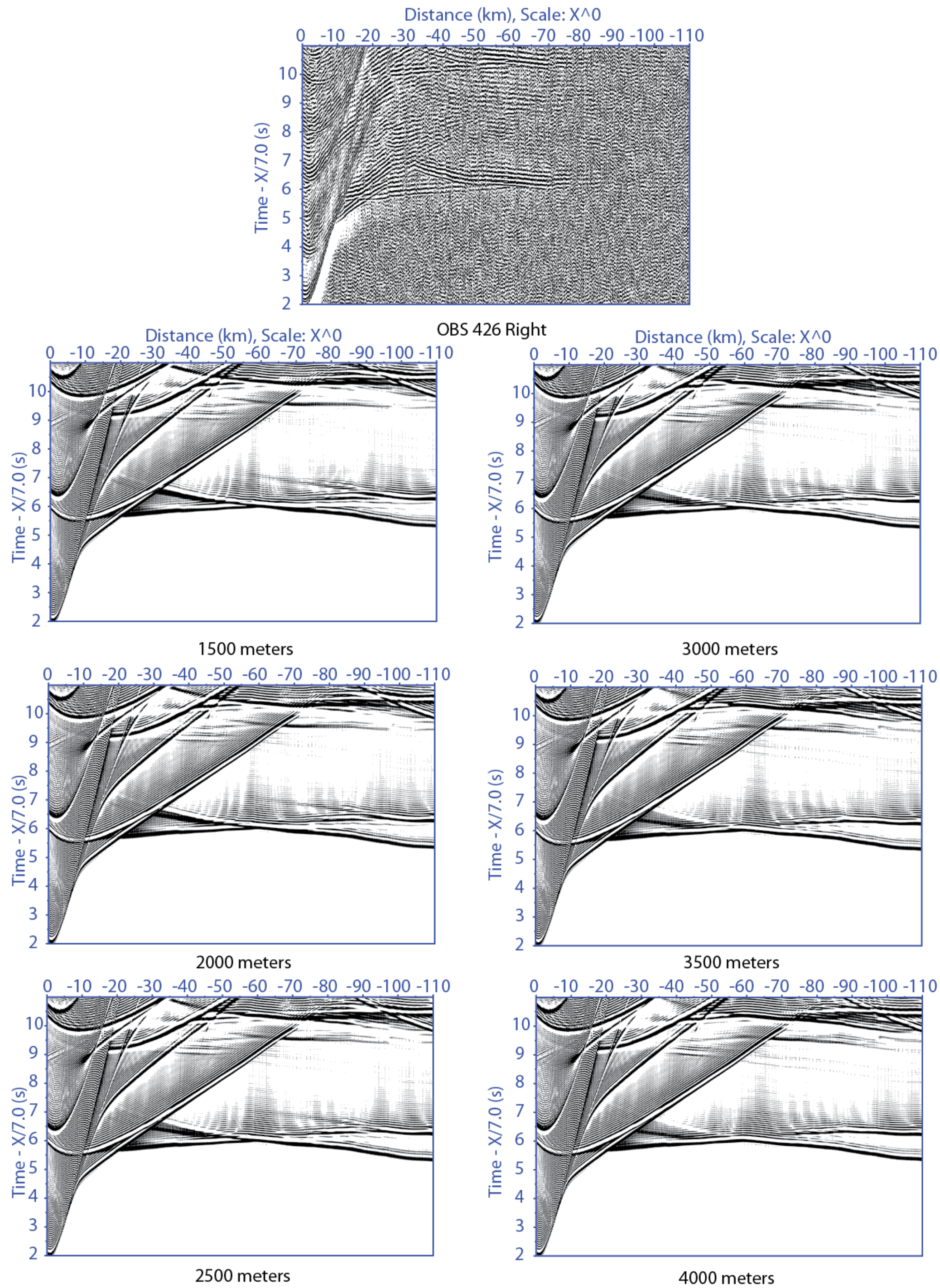

Figure B-7: OBS 426 (left offset) Synthetic Models

Synthetic models for 1500 to 4000 meter crust-mantle transition

References

Assefa, Solomon, Clive McCann, and Jeremy Sothcott. "Velocities Of Compressional And Shear Waves In Limestones." *Geophysical Prospecting* 51.1 (2003): 1-13.

Bakulin, A. , F. Kets, M. Hauser, R. Vines, and J. Wieseneck, 2008, Influence of horizontal and vertical stresses on Vp-Vs trends: 78th Annual International Meeting, SEG, Expanded Abstracts, 1625-1628

Bird, et al. "Gulf Of Mexico Tectonic History; Hotspot Tracks, Crustal Boundaries, And Early Salt Distribution." *AAPG Bulletin* 89.3 (2005): 311-328.

Brocher, Thomas M. "Empirical Relations Between Elastic Wavespeeds And Density In The Earth's Crust." *Bulletin Of The Seismological Society Of America* 95.6 (2005): 2081-2092.

Carbonell, R., J. Gallart, and A. Perez-Estaun. "Modelling And Imaging The Moho Transition; The Case Of The Southern Urals." *Geophysical Journal International* 149.1 (2002): 134-148.

Cerveny, V. 2001, Seismic ray theory. Cambridge University Press, Cambridge, U.K

Christensen, Nikolas I. "Poisson's Ratio And Crustal Seismology." *Journal Of Geophysical Research* 101.B2 (1996): 3139-3156.

Cox, K.G. “A Model for Flood Basalt Vulcanism” Journal of Petrology (1980), vol. 21, part 4, pp 629 – 650.

Dickinson, William R. (2009) "The Gulf Of Mexico And The Southern Margin Of Laurentia." *Geology [Boulder]* 37.5 (2009): 479-480.

Dickinson, W. R., G. E. Gehrels, and R. J. Stern (2010), Late Triassic Texas uplift preceding Jurassic opening of the Gulf of Mexico: Evidence from U-Pb ages of detrital zircons, *Geosphere*, *6*, 641-662 doi:10.1130/GES00532.1

Eccles, Jennifer D., Robert S. White, and Philip A. F. Christie. "Identification And Inversion Of Converted Shear Waves; Case Studies From The European North Atlantic Continental Margins." *Geophysical Journal International* 179.1 (2009): 381-400.

Eddy, D.R., H.J.A. van Avendonk, and D.J. Shillington (2013), Compressional and shear-wave velocity structure of the continent-ocean transition zone at the eastern Grand Banks, Newfoundland. Journal of Geophysical Research, in press

Fillon, Richard H. "Mesozoic Gulf Of Mexico Basin Evolution From A Planetary Perspective And Petroleum System Implications." *Petroleum Geoscience* 13.2 (2007): 105-126.

Galloway, W. E., 2008, "Depositional evolution of the Gulf of Mexico sedimentary basin." in K.J. Hsu, ed., pp. 505-549, The Sedimentary Basins of the United States and Canada, Sedimentary Basins of the World. v. 5, Elsevier, The Netherlands.

Gernigon, et al. "The Norway Basin Revisited; From Continental Breakup To Spreading Ridge Extinction." *Marine And Petroleum Geology* 35.1 (2012): 1-19.

Hale, L. D., and G. A. Thompson (1982), The seismic reflection character of the continental Mohorovicic discontinuity, *J. Geophys. Res.*, *87*, 4625- 4635.

Hamilton, E. L. "Vp /Vs And Poisson's Ratios In Marine Sediments And Rocks." *Journal Of The Acoustical Society Of America* 66.4 (1979): 1093-1100.

Heatherington, A.L., and Mueller, P.A., 1999, Lithospheric sources of North Florida, USA, tholeiites and implications for origins of the Suwannee terrane: Lithos, v. 46, p. 215– 233, doi: 10.1016/S0024-4937(98)00063-2.

Heatherington, A.L., and Mueller, P.A., 2003, Mesozoic igneous activity in the Suwannee terrane, southeastern USA: Petrogenesis and Gondwanan affinities: Gondwana Research, v. 6, p. 296–311, doi: 10.1016/S1342-937X (05)70979-5.

Hooper, Peter R. "The Timing Of Crustal Extension And The Eruption Of Continental Flood Basalts." *Nature [London]* 345.6272 (1990): 246-249.

Imbert, P., Cramez, C., Talwani, M., and Jackson, M., 2001, “Seaward-dipping reflectors in the eastern Gulf of Mexico: Implications for basin opening”: Geological Society of America Abstracts with Programs, v.33, no. 6, 157–158.

Imbert, Patrice. "The Mesozoic Opening Of The Gulf Of Mexico; Part 1, Evidence For Oceanic Accretion During And After Salt Deposition." *Program And Abstracts - Society Of Economic Paleontologists. Gulf Coast Section. Research Conference* 25.(2005): 50.

Imlay, R. W. "Jurassic Paleobiogeography Of The Conterminous United States In Its Continental Setting." *U. S. Geological Survey Professional Paper* (1980)

Jarchow, Craig M., and George A. Thompson. "The Nature Of The Mohorovicic Discontinuity." *Annual Review Of Earth And Planetary Sciences*

17.(1989): 475-506.Keiswetter, D., R. Black, and C. Schmeisser (1996), A program for seismic wavefield modeling using finite-difference techniques, *Comput. Geosci.*, *22*, 267-286.

Kelly, K. R., R. W. Ward, S. Treitel, and R. M. Alford (1976), Synthetic seismograms: A finite-difference approach, *Geophysics*, *41*, 2-27.

Kennett, B, Salmon, M, Saygin, E, Rawlinson, N, Pozgay, S, Tkalcic, H, Vanacore, E, Collins, C, Goleby, B, Goncharov, A, Maher, J, Reading, A, Aitken, A, Revets, S, Shibutani, T, Clitheroe, G, Arroucau, P, & Fontaine, F 2011, 'AusMoho; the variation of Moho depth in Australia', *Geophysical Journal International*, 187, 2, pp. 946-958

Klitgord, K. D., P. Popenoe, and H. Schouten (1984), Florida: A Jurassic transform plate boundary, *J. Geophys. Res.*, *89*, 7753–7772.

Mann, Paul. "Overview Of The Tectonic History Of Northern Central America." *Special Paper - Geological Society Of America* 428.(2007): 1-19.

Marzoli et al., et al. "Extensive 200-Million-Year-Old Continental Flood Basalts Of The Central Atlantic Magmatic Province." *Science* 284.5414 (1999): 616-618.

McHone, J. G. "Non-Plume Magmatism And Rifting During The Opening Of The Central Atlantic Ocean." *Tectonophysics* 316.3-4 (2000): 287-296.

Menzies, et al. "Characteristics Of Volcanic Rifted Margins." *Special Paper - Geological Society Of America* 362.(2002): 1-14.

Mickus, et al. "Potential Field Evidence For A Volcanic Rifted Margin Along The Texas Gulf Coast." *Geology [Boulder]* 37.5 (2009): 387-390.

Mooney, W. D., and T. M. Brocher (1987), Coincident seismic reflection/refraction studies of the continental lithosphere: A global view, *Rev. Geophys.*, *25*, 723-742.

Mohorovicic, A. 1910. Das Beben vom 8. X. 1909. Jahrb. Meteorol. Obs. Zagreb. 9. Teil 4. Abschn. I. 63

Oueity, J., and R. M. Clowes. "Nature Of The Moho Transition In NW Canada From Combined Near-Vertical And Wide-Angle Seismic-Reflection Studies." *Lithosphere* 2.5 (2010): 377-396

Pallister, John S., and Clifford A. Hopson. "Samail Ophiolite Plutonic Suite; Field Relations, Phase Variation, Cryptic Variation And Layering, And A Model Of A Spreading Ridge Magma Chamber." *Journal Of Geophysical Research* 86.B4 (1981): 2593-2644.

Pindell, James, and John F. Dewey. "Permo-Triassic Reconstruction Of Western Pangea And The Evolution Of The Gulf Of Mexico/Caribbean Region." *Tectonics* 1.2 (1982): 179-211.

Quick, James E., Silvano Sinigoi, and Adriano Mayer. "Emplacement Of Mantle Peridotite In The Lower Continental Crust, Ivrea-Verbano Zone, Northwest Italy." *Geology [Boulder]* 23.8 (1995): 739-742.

Ross, Malcolm I., and Christopher R. Scotese. "A Hierarchical Tectonic Model Of The Gulf Of Mexico And Caribbean Region." *Tectonophysics* 155.1-4 (1988): 139-168.

Salvador, Amos. "Late Triassic-Jurassic Paleogeography And Origin Of Gulf Of Mexico Basin." AAPG Bulletin 71.4 (1987): 419-451.

Sawyer, Dale S., Richard T. Buffler, and Rex H., Jr. Pilger. "The Crust Under The Gulf Of Mexico Basin The Geology Of North America." 53-72. United States: Geol. Soc. Am. : Boulder, CO, United States, 1991.

Smith, Alan D. "Back-Arc Convection Model For Columbia River Basalt Genesis." *Tectonophysics* 207.3-4 (1992): 269-285.

Stern, R J., and Dickinson W R. "The Gulf Of Mexico Is A Jurassic Backarc Basin." *Geosphere* 6.6 (2010): 739-754.

Todd, T, and Simmons, G. "Effect Of Pore Pressure On The Velocity Of Compressional Waves In Low-Porosity Rocks." *Journal Of Geophysical Research* 77.20 (1972): 3731- 3743.

Urban, et al. "Jurassic Volcanic And Sedimentary Rocks Of The La Silla And Todos Santos Formations, Chiapas; Record Of Nazas Arc Magmatism And Rift-Basin Formation Prior To Opening Of The Gulf Of Mexico." *Geosphere* 7.1 (2011): 121-144.

Van Avendonk, H. J. A., D. J. Shillington, W. S. Holbrook, and M. J. Hornbach (2004), Inferring crustal structure in the Aleutian island arc from a sparse wide-angle seismic data set, Geochem. Geophys. Geosyst., 5, Q08008, doi:10.1029/2003GC000664.

Vetrici, Dan Gr. “Carbonate Reservoirs in Western Canada: an Update.” CREWES Research Report, Volume 5 (1993): 27-1 – 27-24.

Vita

Mark Hamilton Duncan was born in 1980 in Washington D.C. He grew up in both the D.C. area and in Boothbay Harbor, Maine. After high school, he joined the United States Marine Corps in 2001. After being honorably discharged, he began studying geology at Northern Virginia Community College. This led to his increased interest in the subject and eventual acceptance to the University of Arizona in 2007. While attending the U of A, his interests in both geology and mathematics developed into his fascination with geophysics and seismology. In 2011 he was accepted to the University of Texas as a research assistant under the supervision of Gail Christeson. He will begin work at Schlumberger as a seismic data processing engineer in June, 2013.

Email: markhduncan@gmail.com

This thesis was typed by Mark Hamilton Duncan